On the Influence of Constant Vertical Wind Speed on the Classical Ekman Spiral

Sam de Jong

Bachelor End Project 2021

On the Influence of Constant Vertical Wind Speed on the Classical Ekman Spiral

by

Sam de Jong

to obtain the degree of Bachelor of Science
at the Delft University of Technology,
to be defended publicly on Thursday August 5th, 2021 at 2:00 PM.

Student number:	4965396	
Project duration:	April 19, 2021 – August 5, 2021	
Thesis committee:	Dr. ir. W. T. van Horssen,	TU Delft, supervisor
	Dr. ir. K. Cools,	TU Delft
	Dr. ir. W. A. A. M. Bierbooms	TU Delft

TU Delft Delft University of Technology

Abstract

The Ekman spiral is described by a coupled system of differential equations originally discussed by Walfrid Ekman (Ekman, 1905). This system is a simplified version of the Navier-Stokes equations. The differential equations, as discussed in Ekman's paper, concern the currents of the ocean. However, it is also possible to interpret these equations so as to describe and predict the flow of wind.

The research as presented is not only inspired by Walfrid Ekman's original paper, but also by the master thesis from de Jong (2021). The main contribution of this thesis is to include the influence of a constant vertical wind speed on the classical Ekman spiral. After stuyding the classical Ekman spiral, the inclusion of a constant vertical wind speed is done step-wise. First, the vertical wind speed is discussed without having any vertical Coriolis forces. The classical Ekman spiral and the Ekman spiral with vertical wind, but no vertical Coriolis force, were solved exactly. Then, the vertical wind speed is included fully, giving rise to a non-linear coupled system of differential equations.

For the non-linear system, an algorithm for solving it analytically using a general perturbation method is proposed. Next, the hodograph of the non-linear equations of motion including a constant vertical wind speed, is made using Euler's Explicit numerical method and a shooting problem is solved.

Preface

With this bachelor thesis, I present my scientific research on the influence of a constant vertical wind speed on the behaviour of the Ekman spiral. This thesis is written as part of the Bachelor End Project 2020-2021 for graduating applied mathematics students.

This report is intended for readers with a physical and/or mathematical background. The first is useful for understanding the physical interpretation of the wind speeds and the latter is to understand the solution methods used in this thesis.

Readers with a special interest in the results of the Ekman spiral with a constant vertical wind speed can find this in Chapter 5. Readers of this thesis do not need to be familiar with the Ekman spiral, as this will be discussed in Chapter 3. For the general equation of motion used in this thesis, readers are referred to Chapter 2.

Firstly, I would like to thank my supervisor, Wim van Horssen, for his valuable input, time and support during this thesis. His provided insight and relaxed work environment made sure that this thesis came to a good end.

Secondly, I would like to thank Kristof Cools and Wim Bierbooms for taking a seat in my thesis committee.

Lastly, I would like to thank family and friends for their support. Especially, André, Ellen, Gijs, Isa, Joppe and Wouter for proofreading and discussing the thesis.

Delft, July 2021
Sam de Jong

Contents

Nomenclature

Abbreviations

ABL	Atmospheric Boundary Layer
AWEA	American Wind Energy Association
ESA	European Space Agency
ISA	International Standard Atmosphere
RPM	Regular Perturbation Method

Greek symbols

β	Angle between geostrophic wind direction and horizontal component of Earth's rotation [rad]
ε_u	Difference between wind speed u of classical and modified linear spiral [-]
ε_v	Difference between wind speed v of classical and modified linear spiral [-]
$\hat{\varepsilon_u}$	Difference between wind speed u of modified linear Ekman spiral and Ekman spiral with vertical wind speed [-]
$\hat{\varepsilon_v}$	Difference between wind speed v of modified linear Ekman spiral and Ekman spiral with vertical wind speed [-]
λ	Troposphere lapse rate [K/m]
ρ	Air density [kg/m^3]
ϕ	Latitude [rad]
Ω	Angular velocity [rad/s]

Roman symbols

f	Coriolis parameter [rad/s]
$\hat{f}$	Vertical Coriolis parameter [rad/s]
g	Gravitational acceleration [m/s^2]
K_M	Turbulent viscosity [m^2/s]
p	Air pressure [Pa]
P_i	Pressure over air density gradient in i-direction [Pa m^3/kg]
R	Universal gas constant [J/(kg K)]
T_0	Temperature at ground level [K]
t	Time [s]
u	Wind speed in x-direction [m/s]
v	Wind speed in y-direction [m/s]
w	Wind speed in z-direction [m/s]

$\bar{u}$	Geostrophic wind speed [m/s]
$\hat{u}$	Non-dimensional wind speed in x-direction [-]
$\hat{v}$	Non-dimensional wind speed in y-direction [-]
$\hat{w}$	Non-dimensional wind speed in z-direction [-]
z	Height [m]
$\hat{z}$	Non-dimensional height [-]
z_0	Ground level height [m]
z_i	ABL height [m]

List of Figures

List of Tables

1 Introduction

Understanding the flow of wind at great heights is crucial in yielding sustainable wind energy. Wind energy is a popular source of green energy, which is mainly harvested using wind turbines. These operate on the same basic principles of older windmills. There are horizontal-axis and vertical-axis wind mills, which refers to which axis the main rotor shaft is parallel to (AWEA, 2010). The size of the wind turbine may vary, but is crucial for how much energy can be harvested. For both types of these windmills, a strong wind is crucial for yielding energy (Roussey, 2021). A greater height of the turbine implies a greater energy yield, as there is stronger wind flow at greater heights. However, this does make the turbine more expensive, as it needs to be able to withstand these strong wind flows. Generally speaking, the size of wind turbines has increased steadily over the last years (AWEA, 2010).

As the wind turbines increase in height every year, it is important to have a thorough analysis of the wind flows at great heights. Nowadays, the equations of motion derived by Walfrid Ekman, discussed in his paper (Ekman, 1905), are used to determine the wind flow at great heights. A major shortcoming in his equations of motion is the assumption that there is no vertical wind speed. This imperfection was previously not a problem, as the vertical wind speed did not have a significant influence on the structure of wind turbines. However, the call for a more accurate evaluation, including vertical wind speeds, has recently started so that even more wind energy can be yielded.

A better analysis of the flow of wind at greater heights will have a big impact on wind turbines. This new evaluation on Ekman's equations of motion will make sure that each turbine will be constructed both cost-efficiently and even more structurally sound. Hence, even more wind energy will be yielded, which lays the groundwork of working towards a sustainable, reliable and environmentally friendly future.

The aim of the thesis is to derive and solve three different versions of Ekman's spiral, each being different in allowing vertical wind speed. This thesis is inspired by a previous thesis (de Jong, 2021), specifically on the Ekman Spiral. First, the classical Ekman spiral (Ekman, 1905) will be derived and solved. Then, a modified linear version of the classical spiral will also be solved. Lastly, the focus is put on the classical Ekman spiral, but now considering a constant wind speed moving in vertical direction.

In this thesis, there are two objectives. The first objective is to follow through the calculations made in the previous work by de Jong (2021) and extend it by satisfying the imposed boundary conditions exactly. The previous thesis worked out a version of Ekman's spiral which allowed constant vertical wind speed but no vertically acting Coriolis force. This version is called the modified linear Ekman spiral.

Secondly, this thesis aims to be an extension of the modifications done on the Ekman Spiral. This is done via adding modifications to the Ekman Spiral through non-linear variations, solving these numerically using the explicit Euler method. This serves to give a better understanding on the behaviour of wind in great heights.

This report has the following structure. First, in Chapter 2 the equation of motion from the atmospheric Navier-Stokes equations are derived. The atmospheric Navier-Stokes equations were in turn derived in the book by Emeis (2018). The special case of solving the equations from Walfrid Ekman is done

in Chapter 3. The modified Ekman Spiral, as dicussed by de Jong (2021), is discussed and solved in Chapter 4. Thereafter, the equations of motion including a constant vertical wind speed are discussed, an algorithm is given to solve the equations of motion analytically using a general perturbation method, and numerically visualized in Chapter 5. Lastly, in Chapter 6 a conclusion on this thesis and several recommendations for further research into this subject are given.

2

Equations of Motion

In this chapter, the equations of motion for Ekman's Spiral are derived from the atmospheric Navier-Stokes equations given by Emeis (2018) together with the boundary conditions. Firstly, the coordinate system for the Navier-Stokes equations is introduced in Section 2.1. Following, the equations of motion for the Ekman Spiral are derived in Section 2.2. Several assumptions on these equations are made in Section 2.3 so as to simplify the system. After that, final equations of motion which are discussed in this report are shown in Section 2.4. Different boundary conditions which will have to be satisfied together with the aforementioned equations of motion are discussed in Section 2.5. This chapter is concluded by Section 2.6, where the values of parameters given in the Navier-Stokes equations and boundary conditions are discussed.

2.1. Coordinate system for Navier-Stokes Equations

Before the Navier-Stokes equations are introduced, it is important to define the coordinate system that is used in this thesis. The following image shows the system used.

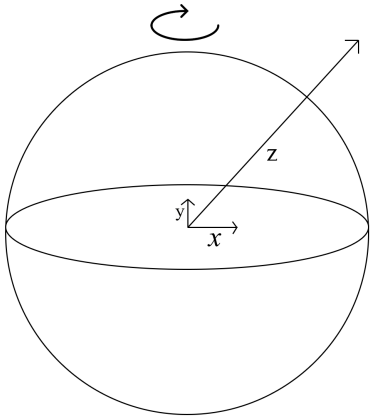

Figure 2.1: The coordinate system used for the Navier-Stokes equations, indicated on a side view of the Earth.

In Figure 2.1, the arrow above the globe represent the direction of rotation. The latitude is defined as the angle between the z- and x-axis.

2.2. Atmospheric Navier-Stokes Equations

Wind flowing in the atmospheric boundary layer can be described using the following set of vector equations. These are derived from the Navier-Stokes equations (Doering and Gibbon, 1995) and are given in Equation (2.1) and Equation (2.2). Equation (2.1) describes the flow of a fluid or gas. Note that Equation (2.2) represents the continuity equation, which can be physically interpreted as the conservation

of volume (Parker, 2003)

$$\frac{\partial \mathbf{u}}{\partial t} + \mathbf{u} \cdot \nabla \mathbf{u} + \frac{1}{\rho} \nabla \mathbf{p} = 2\Omega \times \mathbf{u} + K_M \nabla^2 \mathbf{u} + \mathbf{g}, \tag{2.1}$$

$$\nabla \cdot \mathbf{u} = 0. \tag{2.2}$$

Several variables in Equation (2.1) and Equation (2.2) will now be explained. First, the vector $\mathbf{u}$ has three components: u, v and w which represent the wind speed in the x, y and z direction respectively. Variable t represents the time. The air density in this equation is ρ, and the pressure is $\mathbf{p}$. Then, Ω represents the rotation of the earth, K_M represents the turbulent viscosity and $\mathbf{g}$ is the gravitational constant.

The time-dependency is denoted by the first fraction, $\frac{\partial \mathbf{u}}{\partial t}$. As the flow might accelerate, the term $\mathbf{u} \cdot \nabla \mathbf{u}$ denotes the convective acceleration. Variable $\mathbf{p}$ represents the pressure. This means that $\frac{1}{\rho} \nabla \mathbf{p}$ will represent the pressure gradient force. The term $2\Omega \times \mathbf{u}$ represent the Coriolis force. Then, the term $K_M \nabla^2 \mathbf{u}$ is the friction force on the fluid. Lastly, $\mathbf{g}$ captures the effect of the gravitational force.

Having clarified all the different variables in Equation (2.1) and Equation (2.2), Section 2.3 will discuss the different assumptions made to simplify.

2.3. Assumptions on Navier-Stokes Equations

To simplify Equation (2.1) and Equation (2.2), certain assumptions are made when analysing the flow of the wind. These assumptions are discussed in this section.

Firstly, it is assumed that the gravity is constant both with respect to time and space. In reality, gravitation varies per location on the globe, but this variation is negligible.

Next, the wind speed is assumed to be constant in time. That is, a steady flow is considered. Therefore the term $\frac{\partial \mathbf{u}}{\partial t}$ can be omitted. In reality, the wind speed will vary in time.

Thirdly, there is assumed to be no variation in direction of the wind in $x-$ and $y-$direction. In reality, this may occur but for the sake of simplicity it is assumed that the variation is negligible.

Both the pressure and density are assumed to change according to the International Standard Atmosphere (ISA) (Anderson-Jr, 1978). Both change with respect to height, conform to the ISA with the following relation shown in Equation (2.3) and Equation (2.4)

$$\rho(z) = \rho_0 \left(1 + \frac{\lambda_0}{T_0} z\right)^{-\frac{g}{R\lambda_0} - 1}, \tag{2.3}$$

$$p(z) = p_0 \left(1 + \frac{\lambda_0}{T_0} z\right)^{-\frac{g}{R\lambda_0}}. \tag{2.4}$$

In the above equations, z represents the height as denoted in Section 2.1. Parameters ρ_0 and p_0 represent the density and pressure at ground level, $z = 0$, respectively. λ_0 is the lapse rate in the troposphere, and T_0 is the temperature at ground level. R indicates the universal gas constant. Having constant density and pressure means that parameter K_M remains constant as well.

The air is assumed to be incompressible. This means that air is assumed to be incapable of or resistant to compression. This might not be the case in reality.

2.4. Equations of Motion

Having implemented the aforementioned assumptions, the equations of motion in Equation (2.1) and Equation (2.2) become Equation (2.5)

$$\begin{aligned} w \cdot u_z + P_x &= 2v\Omega \sin\phi - 2w\Omega \cos\phi \sin\beta + K_M u_{zz}, \\ w \cdot v_z + P_y &= 2w\Omega \cos\phi \cos\beta - 2u\Omega \sin\phi + K_M v_{zz}, \\ w \cdot w_z + P_z &= K_M w_{zz} - g. \end{aligned} \tag{2.5}$$

Three new parameters are introduced in this equation. The first parameter P simply equals $\frac{p}{\rho}$, the pressure gradient divided by the air density, whereas the second parameter β coincides with the following

Equation (2.6). Note that β depends on both horizontal wind speeds in the following way:

$$\tan\beta = \frac{v}{u}. \tag{2.6}$$

The last parameter is ϕ, which is used to denote the latitude. Equation (2.5) and Equation (2.6) will later be used for further analysis, but first the equations for Ekman Spiral will be derived.

Note that in Equation (2.5) the cross-product concerning the Coriolis force has been written out. This is done due to the equations being easily simplified in future sections. The influence of the Coriolis force on the equation of motion concerning the vertical wind speed is equal to zero, which can be shown by using the trigonometric relations of both the sine and cosine of the arc-tangent.

2.5. Boundary Conditions imposed on Equations of Motion

To solve the above mentioned equations of motion, boundary conditions are required. It is assumed that there is a boundary condition at the ground level, so $z = z_0$, and a boundary condition at the top height, $z = z_i$, which is the top height of the atmospheric boundary layer (ABL). These differ from Walfrid Ekman's (Ekman, 1905) original boundary conditions, as he discussed the problem on a sea surface. Walfrid Ekman had a lower boundary at $z = -\infty$ and an upper boundary at $z = 0$. As now the wind flow is studied, the boundary is shifted.

At the lower level, the wind speed is assumed to be negligible. This means that the wind speed vector will be equal to the zero vector. Hence, there will be no slip. Also, the ground level height, indicated by parameter z_0, will be set equal to 0.

At the higher level, there is assumed to be a geostrophic wind. The direction of the geostrophic wind is perpendicular to both the pressure gradient force and the Coriolis force, chosen to be in the direction of the x-axis. Hence, the uppper boundary condition will be at height z_i and have $u = \bar{u}$ and $v = 0$,

2.6. Values of Parameters

This section discussed the parameters and boundary conditions imposed on the equations of motion. The different parameters are given in Equation (2.5) and discussed in the boundary conditions imposed in Section (2.5).

The first parameter that will be discussed is the geostrophic wind speed. The geostrophic wind speed, $\bar{u}$, which is the value of the wind speed on the upper boundary condtions, is assumed to be ten metres per second. The speed depends on the pressure, density, the rotation of the earth and latitude (Hakim and Holton, 2012).

The other parameter discussed in Section 2.5 is the height of the atmospheric boundary layer. This height, indicated with parameter z_i, is taken to be 1000 metres. It might vary between 1000 and 2500 metres (Emeis, 2018).

The first parameter in Equation (2.5) will be the vertical wind speed w, as it is assumed to be constant. Generally speaking, it will not be constant. The value of the vertical wind speed is assumed to be 0.0025 metres per second. The wind speed might also take values in between -2 and 2 metres per second (Zhang et al., 2019).

Next, the rotational speed of the earth is discussed. Parameter Ω is assumed to be equal to $7.27 \cdot 10^{-5}$ radians per second (Elert, 2009).

The latitude of the location that is studied is also a parameter in Equation (2.5). The latitude in the Netherlands is equal to 52 degrees (MapsOfWorld, 2017). Hence, the parameter ϕ is set equal to 52 degrees.

The parameter indicating the viscosity, is K_M. The value of this parameter varies in between 0.1 and 2000 m^2 per second. It is assumed that this parameter will equal 5 m^2 per second.

The last parameter is gravity contant g. It was already noted that the gravity was assumed to be constant. The value of the gravitational constant can be from 9.78 up to 9.83 metres per s^2, as determined by the European Space Agency (ESA) (ESA, 2021), but in this report is assumed to be equal to 9.81 metres per s^2.

3

Classical Ekman Spiral

This chapter focuses on the derivation and solving of the classical Ekman Spiral. The first section of this chapter will focus on a short derivation of Walfrid Ekman's (Ekman, 1905) spiral equations from the equations of motion obtained in Chapter 2. Following that, Section 3.2 will delve into the process of solving these equations, which is divided into solving for wind speed v and u. Section 3.3 will be the preleminary section of this chapter, a visualization of the spiral and remarks about the properties of the parameters which influence the spiral are given. Lastly, Section 3.4 will conclude this chapter with a short summary and conclusion on the parameters, assumptions and boundary conditions of the classical Ekman spiral.

3.1. Classical Ekman Spiral

For the Ekman Spiral originally discussed by Walfrid Ekman, more assumptions are made on Equation (2.5). Only the pressure gradient force, the Coriolis force and the friction force are considered. Therefore, the gravitational force is neglected. Additionally, the assumption is made that there is no vertical wind speed. Hence, the previous discussed equations of motion, stated in Equation (2.5), can be reduced to the following

$$\begin{aligned} P_x &= 2v\Omega \sin\phi + K_M u_{zz}, \\ P_y &= -2u\Omega \sin\phi + K_M v_{zz}. \end{aligned} \tag{3.1}$$

Note that in Equation (3.1) there is no longer an equation for the wind speed in vertical direction. This is due to the fact that this will transform into the following Equation (3.2).

$$P_z = K_M w_{zz}|_{z=0} = C, \tag{3.2}$$

with C being a constant. This gives that the pressure gradient divided by the air density with derivative taken with respect to x or y will be constant with height.

In Equation (3.1), the term $2\Omega \sin\phi$ is actually constant, which will thus be called f from now on, the Coriolis parameter. This constant is shown in Equation (3.3)

$$f = 2\Omega \sin\phi. \tag{3.3}$$

In the original Equation (2.5), there also is a term which contains a cosine instead of a sine in the Coriolis parameter. This slightly modified parameter is defined in Equation (3.4). It is defined to be the vertical component of the Coriolis force

$$\hat{f} = 2\Omega \cos\phi. \tag{3.4}$$

The value of these parameters will be the following

$$f = 2 \cdot 7.27 \cdot 10^{-5} \cdot \sin(52) = 1.1 \cdot 10^{-4}, \tag{3.5}$$

and

$$\hat{f} = 2 \cdot 7.27 \cdot 10^{-5} \cdot \cos(52) = 0.9 \cdot 10^{-4}. \tag{3.6}$$

The parameters and their values used to calculate both Coriolis parameters were discussed in Section 2.6. Parameter $\hat{f}$ is not used in this chapter, but will be used later in Chapter 5.

The set of equations given in Equation (3.1) require boundary conditions. These are discussed in Section 2.5. However, the boundary conditions that Ekman imposed in his paper (Ekman, 1905), are different from those as discussed in Section 2.5. In short, to coincide with the boundary conditions taken in his paper, the boundary conditions are changed slightly. Both the upper and lower boundary are shifted up by an infinite height. Thus the lower boundary will be at ground level, $z = 0$. The upper boundary will be at infinite height. There, it is assumed that there is only a constant geostrophic wind $\bar{u}$, which is pointed in the direction of wind speed u.

Filling in the last boundary condition into Equation (3.1), gives Equation (3.7)

$$\begin{aligned} P_x &= 0, \\ P_y &= -f\bar{u}. \end{aligned} \tag{3.7}$$

As both P_x and P_y were constant with height, these values can directly be substituted into Equation (3.1). Also adding the previously discussed constant f, gives Equation (3.8)

$$\begin{aligned} -fv &= K_M u_{zz}, \\ fu - f\bar{u} &= K_M v_{zz}. \end{aligned} \tag{3.8}$$

Having derived this coupled system of differential equations, the following section will focus on solving them.

3.2. Solving Classical Ekman Spiral

This section focuses on solving the coupled differential equations as obtained in the previous Section 3.1. First the solution for wind speed v will be discussed. Then, using the coupled differential equations, the solution for wind speed u will be obtained.

Equation (3.8) can be separated into two fourth-order differential equations. This is done by differentiating both equations with respect to height z, then substituting them into each other

$$\begin{aligned} -fv &= \frac{K_M^2}{f} v_{zzzz}, \\ fu - f\bar{u} &= -\frac{K_M^2}{f} u_{zzzz}. \end{aligned} \tag{3.9}$$

A constant ϵ is introduced, having the following value:

$$\epsilon = \frac{K_M}{f} \tag{3.10}$$

Substituting the constant ϵ into Equation (3.9), gives the following

$$\begin{aligned} -v &= \epsilon^2 v_{zzzz}, \\ u - \bar{u} &= \epsilon^2 u_{zzzz}. \end{aligned} \tag{3.11}$$

The first equation of Equation (3.11) can now be solved. Having $v(z)$, one can determine $u(z)$ by merely differentiating it and substituting it into the second equation in original Equation (3.8).

The characteristic equation, by trying a solution $v(z) = \mathrm{e}^{rz}$ with r a constant, is the following:

$$\epsilon^2 r^4 = -1 \qquad \Rightarrow \qquad (\sqrt{\epsilon} r)^4 = -1 \tag{3.12}$$

The last step in deriving the value of r for the characteristic equation requires some complex function analysis. In short, it holds true that

$$\sqrt{\epsilon} r = \pm \frac{1}{\sqrt{2}}(1 + i), \qquad \text{or} \qquad \sqrt{\epsilon} r = \pm \frac{1}{\sqrt{2}}(-1 + i). \tag{3.13}$$

Having the value of the complex numbers and therefore the value of r, the solution is therefore the following sum

$$v(z) = \mathrm{e}^{\frac{z}{\sqrt{2\epsilon}}}\left(d_1 \cos\left(\frac{z}{\sqrt{2\epsilon}}\right) + d_2 \sin\left(\frac{z}{\sqrt{2\epsilon}}\right)\right) + \mathrm{e}^{-\frac{z}{\sqrt{2\epsilon}}}\left(d_3 \cos\left(\frac{z}{\sqrt{2\epsilon}}\right) + d_4 \sin\left(\frac{z}{\sqrt{2\epsilon}}\right)\right). \tag{3.14}$$

Note that the solution for horizontal wind speed v still has four constants, these will be determined using the boundary conditions in the following section.

3.2.1. Boundary Conditions imposed on Specific Wind Speed

Solving the Equation (3.14) requires boundary conditions. There are two boundary conditions, as discussed before. For equation concerning the wind speed v, there are two boundary conditions readily available. These were discussed in Section 3.1 and given generally in Section 2.5. At ground level, $z = 0$, there is no wind speed, hence $v = 0$. Also, at infinite height, $z \to \infty$, there is geostrophic wind, which is not in the direction of v, so also here it will hold that $v = 0$.

However, as there are four constants, also four boundary conditions are needed. The last two are obtained by substituting the boundary conditions for wind speed u into Equation (3.8). For the ground speed boundary condition, the following is obtained

$$-\bar{u} = \epsilon v_{zz}(0). \tag{3.15}$$

For the boundary conditions at infinite height, the last boundary condition will be

$$0 = \epsilon v_{zz}(z) \qquad \text{for } z \to \infty \tag{3.16}$$

3.2.2. Solution for Specific Wind Speed

Now that the boundary conditions are determined, Equation (3.14) can be solved. Firstly, using the fact that $v = 0$ at $z = 0$ gives $d_1 + d_3 = 0$. Through the boundary condition at $z \to \infty$, it follows that $d_1 = 0 = d_2$, as the solution cannot go to infinity. Therefore, it is known that also $d_3 = 0$ will hold. Having the values of all the constants, Equation (3.14) can be reduced to

$$v(z) = \mathrm{e}^{-\frac{z}{\sqrt{2\epsilon}}} d_4 \sin\left(\frac{z}{\sqrt{2\epsilon}}\right). \tag{3.17}$$

For the second boundary condition, wind speed v must be differentiated twice with respect to the height z. Thus,

$$v_z(z) = -d_4 \frac{1}{\sqrt{2\epsilon}} \mathrm{e}^{-\frac{z}{\sqrt{2\epsilon}}} \sin\left(\frac{z}{\sqrt{2\epsilon}}\right) + d_4 \frac{1}{\sqrt{2\epsilon}} \mathrm{e}^{-\frac{z}{\sqrt{2\epsilon}}} \cos\left(\frac{z}{\sqrt{2\epsilon}}\right). \tag{3.18}$$

When another derivative with respect to z is taken, all terms containing a sine will drop out. Hence, the derivative of wind speed v twice with respect to the height will be

$$v_{zz}(z) = -2d_4 \left(\frac{1}{\sqrt{2\epsilon}}\right)^2 \mathrm{e}^{-\frac{z}{\sqrt{2\epsilon}}} \cos\left(\frac{z}{\sqrt{2\epsilon}}\right). \tag{3.19}$$

Note that the constant terms in this equation can be simplified to:

$$-2d_4 \left(\frac{1}{\sqrt{2\epsilon}}\right)^2 = -d_4 \left(\sqrt{2}\frac{1}{\sqrt{2\epsilon}}\right)^2 = -d_4 \left(\frac{1}{\sqrt{\epsilon}}\right)^2 = -d_4 \frac{1}{\epsilon} \tag{3.20}$$

Therefore, substituting Equation (3.20) into Equation (3.19) gives the total derivative of

$$v_{zz}(z) = -\frac{d_4}{\epsilon} \mathrm{e}^{-\frac{z}{\sqrt{2\epsilon}}} \cos\left(\frac{z}{\sqrt{2\epsilon}}\right). \tag{3.21}$$

Using the boundary condition at ground level in the above equation gives that constant $d_4 = \bar{u}$. Therefore, the wind speed will be

$$v(z) = \bar{u} \mathrm{e}^{-\frac{z}{\sqrt{2\epsilon}}} \sin\left(\frac{z}{\sqrt{2\epsilon}}\right). \tag{3.22}$$

And thus, substituting the value for constant ϵ, the following is obtained

$$v(z) = \bar{u} \mathrm{e}^{-\frac{z\sqrt{f}}{\sqrt{2K_M}}} \sin\left(\frac{z\sqrt{f}}{\sqrt{2K_M}}\right). \tag{3.23}$$

3.2.3. Solution for Remaining Wind Speed

As mentioned before in Section 3.2, using Equation (3.8), wind speed u can now be determined. The second derivative of wind speed v with respect to the height z has already been determined in Equation (3.21). Hence, the following is obtained:

$$u(z) - \bar{u} = \epsilon v_{zz} = \epsilon \frac{\bar{u}}{\epsilon} \mathrm{e}^{-\frac{z}{\sqrt{2\epsilon}}} \cos\left(\frac{z}{\sqrt{2\epsilon}}\right). \tag{3.24}$$

Substituting constant epsilon, the equation for wind speed u is obtained

$$u(z) = \bar{u} - \bar{u} \mathrm{e}^{-\frac{z\sqrt{f}}{\sqrt{2K_M}}} \cos\left(\frac{z\sqrt{f}}{\sqrt{2K_M}}\right). \tag{3.25}$$

3.3. Visualization of the Ekman Spiral

A hodograph is made of the wind speed v and u, as seen in Equation (3.23) and Equation (3.25). The hodograph can be seen in Figure 3.1 and Figure 3.2.

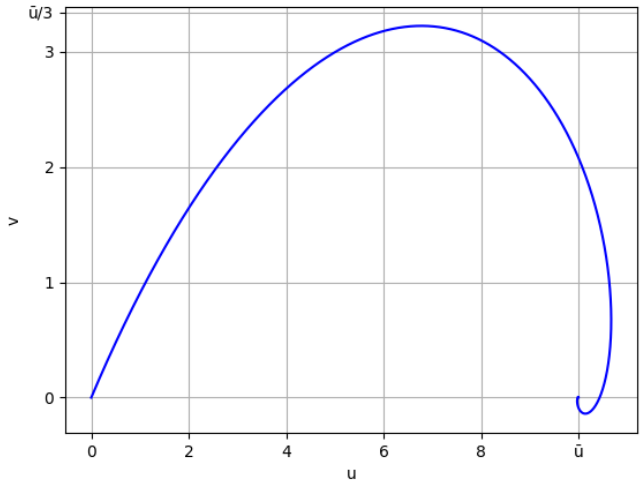

Figure 3.1: A hodograph of the classical Ekman Spiral with parameters $\bar{u} = 10$, $f = 1.1 \cdot 10^{-4}$ and $K_M = 5$.

Note that the figure takes a spiral-like form, hence why it is called the Ekman spiral. There are three parameters which determine the behaviour of the hodograph. The influence of these parameters is discussed individually.

For the further analysis of each parameter Figure 3.2 will be used.

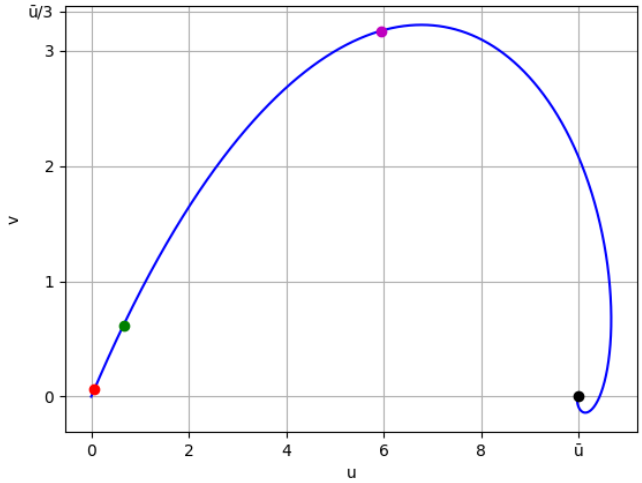

Figure 3.2: A hodograph of the classical Ekman Spiral with parameters $\bar{u} = 10$, $f = 1.1 \cdot 10^{-4}$ and $K_M = 5$ with dots on the graph indicating certain values for the height.

In Figure 3.2, four dots can be seen. The red dot indicates a height of ten. The green dot represents a height of 100 metres, the purple dot a height of 1000 metres and the black dot is put at a height of 10000 metres. These dots are placed at these heights to discuss the influence of the height of the ABL for different parameter values.

The Python code used to visualize above figures and the remaining figures in this chapter can be found in Appendix C.

3.3.1. Influence of the geostrophic wind speed

As indicated already in Figure 3.1 with the ticks on both the u and v axes, the geostrophic wind has a substantial influence on the shape of the classical Ekman spiral. The following two figures both have different values for the geostrophic wind.

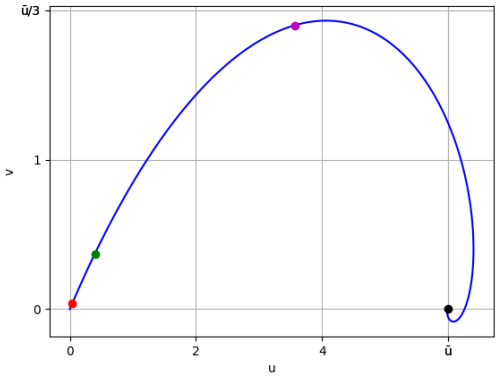

Figure 3.3: A hodograph of the classical Ekman Spiral with parameters $\bar{u} = 6$, $f = 1.1 \cdot 10^{-4}$ and $K_M = 5$.

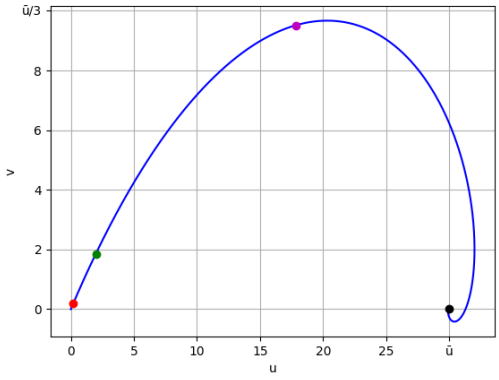

Figure 3.4: A hodograph of the classical Ekman Spiral with parameters $\bar{u} = 30$, $f = 1.1 \cdot 10^{-4}$ and $K_M = 5$.

In Figure 3.3 it can be seen that the shape of the spiral remains the same, but it is scaled by a factor $\frac{4}{5}$ when comparing it to Figure 3.1. The same can be said for Figure 3.4. However, this image is scaled by a factor three when comparing it to Figure 3.1.

Note that the position of the four dots have not changed when comparing to Figure 3.2.

3.3.2. Influence of the Coriolis parameter

The Coriolis parameter has an influence on the speed with which the hodograph goes towards the end point where u is equal to the geostrophic wind speed and v is equal to zero. The figures below each have a different value for the Coriolis parameter as opposed to Figure 3.2.

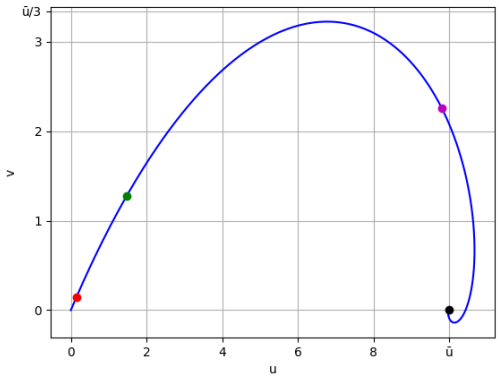

Figure 3.5: A hodograph of the classical Ekman Spiral with parameters $\bar{u} = 10$, $f = 1.1 \cdot 10^{-3}$ and $K_M = 5$.

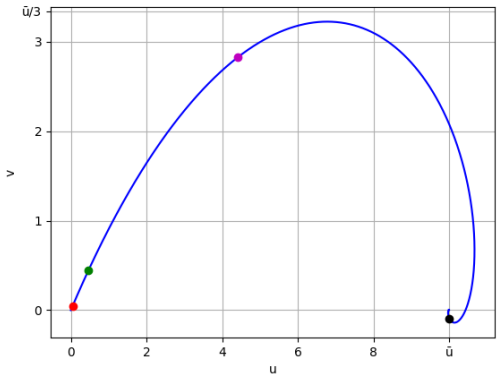

Figure 3.6: A hodograph of the classical Ekman Spiral with parameters $\bar{u} = 10$, $f = 1.1 \cdot 10^{-5}$ and $K_M = 5$.

In Figure 3.5 it can be seen that the dots have moved forward, especially the purple dot. This indicates that the hodograph moves to the geostrophic wind speed for a lower ABL with a bigger Coriolis parameter. For Figure 3.6, it is the exact opposite. The dots have all moved back, meaning that the hodograph moves towards the end point at a higher ABL height.

Also, it can be noted that the figure has not been scaled whatsoever, like previously happened when studying the influence of the geostrophic wind.

3.3.3. Influence of the viscosity

The last parameter that influences the behaviour of the hodograph is the parameter which indicates the viscosity of the fluid. The values of parameter K_M is varied in the two figures below.

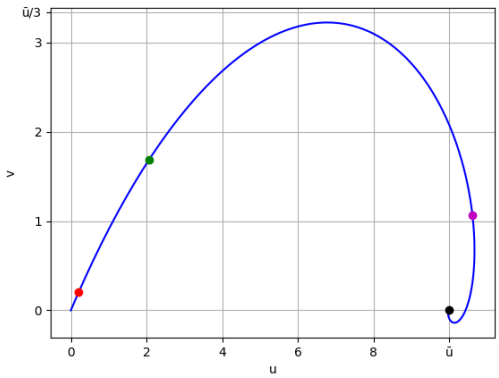

Figure 3.7: A hodograph of the classical Ekman Spiral with parameters $\bar{u} = 6$, $f = 1.1 \cdot 10^{-4}$ and $K_M = 1$.

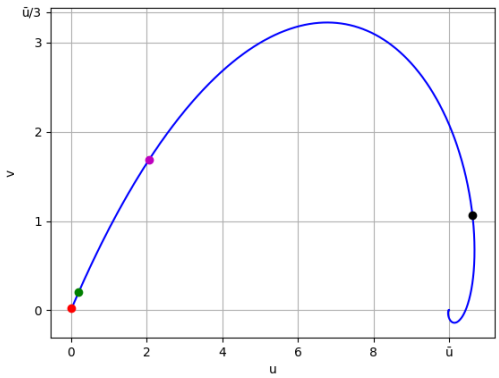

Figure 3.8: A hodograph of the classical Ekman Spiral with parameters $\bar{u} = 30$, $f = 1.1 \cdot 10^{-4}$ and $K_M = 10$.

A similar effect compared to the analysis of the Coriolis parameter f can be seen when studying the above figures. In Figure 3.7 it can be seen that the hodograph for a lower viscosity parameter value reaches the end point for a lower ABL height, while in Figure 3.8 the opposite happens for a bigger viscosity parameter. In Figure 3.8 especially, it can be seen that the black dot has changed position heavily. Thus, it can again be concluded that the value of the viscosity parameter influences the height of the ABL.

Again, no change in the scale happens when studying the influence of this parameter.

3.4. Conclusion on Analysis of Classical Ekman Spiral

This section concludes the chapter on the classical Ekman spiral by giving a short overview of the assumptions, boundary conditions and different parameters.

First, the assumptions for the classical Ekman spiral are discussed. The many assumptions made, especially the assumption that there is no vertical wind speed, impacts how realistic the outcome for the wind flow is. The assumption that there is no gravitational force does not have a major influence on the model.

Second, the boundary conditions discussed in Section 3.2.1 are not realistic as well. Having a boundary at infinite height is a challenge to numerically implement to visualize the hodograph, due to the computational power required to handle larger numbers.

Third, the several parameters discussed in Section 3.3 each play an important role in the behaviour of the hodograph. The speed of the geostrophic wind scales the classical Ekman spiral, which can be attributed to both solutions for wind speed v and u, given in Equation (3.23) and (3.25) respectively, are multiplied with this parameter. The effect of the remaining parameters, the Coriolis parameter and the turbulent viscosity, can be discussed by discussing parameter ϵ, which was defined in Equation (3.10). This parameter influences the height at which the hodograph reaches the end point, a higher ϵ indicated a lower height for the end point and vice versa. This can be associated to the parameter being in the exponent of the solution for wind speed v and u.

In conclusion, the classical Ekman spiral is a simple yet effective way of studying the flow of wind. By rewriting the boundary conditions imposed in Ekman's original paper (Ekman, 1905), an efficient model is created for studying the wind flow. This model is influenced by only two parameters, the geostrophic wind speed and an ϵ, containing the Coriolis parameter and the turbulent viscosity. Both parameters each have a clear and distinct effect on the hodograph produced by implementing the solutions for wind speed v and u.

4

Modified Linear Ekman Spiral

In this chapter, focus is put on a modified linear Ekman spiral. The modified linear Ekman spiral will be introduced in Section 4.1 and the equations of motion will be determined. Then, for the sake of simplicity, the equations of motion obtained in Section 4.1 will be non-dimensionalized in Section 4.2. Thereafter, the non-dimensional equations of motion will be solved in Section 4.3. In Section 4.4, a visualization of the solution posed in the previous section is given. Following that, in Section 4.5, numerical remarks about the visualization and solution of the modified linear Ekman spiral is given. Lastly, in Section 4.6, a conclusion on the analysis of the modified linear Ekman spiral is given. This conclusion concerns the assumptions, boundary conditions, influence on the parameters and the numerical remarks.

4.1. Modified Linear Ekman Spiral

In Ekman's original paper (Ekman, 1905), the assumption was made that there was no vertical wind speed, indicated by variable w. However, in reality there will be such a vertical wind speed. This will change previously discussed equations of motion given in Equation (3.1) into the Equation (4.1).

In this equation, for the sake of linearity, the term given in Equation (3.4) is taken equal to 0. This means that there will be no vertical component of the Coriolis force. The non-linear case is studied in Chapter 5.

The new equations of motion are obtained by taking Equation (2.5) and substituting the Coriolis parameter given in Equation (3.3), discussed in Chapter 3

$$\begin{aligned} w \cdot u_z + P_x &= vf + K_M u_{zz}, \\ w \cdot v_z + P_y &= -uf + K_M v_{zz}. \end{aligned} \tag{4.1}$$

Note that there is no equation concerning the vertical wind speed. This is due to the fact that the vertical wind speed is assumed constant, as this reduces the amount of equations in Equation (4.1) from three to two equations. In reality this vertical wind speed might vary in height.

4.2. Non-dimensionalization

This section will focus on making the equations of motion given in Equation (4.1) non-dimensional.

Via the same argument given in Chapter 3, the pressure gradient divided by the air density with derivative taken with respect to either x or y will remain constant with height. Therefore, values given in Equation (3.7) will be substituted into the above Equation (4.1)

$$\begin{aligned} w \cdot u_z &= vf + K_M u_{zz}, \\ w \cdot v_z - f\bar{u} &= -uf + K_M v_{zz}. \end{aligned} \tag{4.2}$$

The above mentioned equation will now be non-dimensionalized. This will be done in the following sections.

Non-dimensionalization of the Height

The height is the most important variable in the equations of motion, as each derivative is taken with respect to the height z. To non-dimensionalize this variable, it is divided by the atmospheric boundary layer (ABL) height z_i. The non-dimensional height $\hat{z}$ is given in Equation (4.3)

$$\hat{z} = \frac{z}{z_i}. \tag{4.3}$$

Non-dimensionalization of the Wind Speed

The components of the wind speed, u, v and w, will be non-dimensionalized by dividing them by the geostrophic wind speed $\bar{u}$, which has been discussed in previous section. The components without dimension can be seen in Equation (4.4)

$$\begin{aligned} \hat{u} &= \frac{u}{\bar{u}}, \\ \hat{v} &= \frac{v}{\bar{u}}, \\ \hat{w} &= \frac{w}{\bar{u}}. \end{aligned} \tag{4.4}$$

As the equations of motion contain the derivatives of these wind speeds, the derivative needs to be determined. This is done in Equation (4.5)

$$\frac{\mathrm{d}u}{\mathrm{d}z} = \frac{\bar{u}}{z_i}\frac{\mathrm{d}\hat{u}}{\mathrm{d}\hat{z}}. \tag{4.5}$$

As the equations of motion also contain the second derivative with respect to the height, this is determined as well in Equation (4.6)

$$\frac{\mathrm{d}^2u}{\mathrm{d}z^2} = \frac{\bar{u}}{z_i^2}\frac{\mathrm{d}^2\hat{u}}{\mathrm{d}^2\hat{z}}. \tag{4.6}$$

By the same reasoning the new derivative for wind speed v can be determined.

Non-dimensional Boundary Conditions

The boundary conditions were discussed generally in Section 2.5. As they play an important part in solving the equations of motion, they need to be non-dimensionalized as well. The boundary conditions imposed on the system were

$$\begin{aligned} u(0) &= 0, \qquad u(z_i) = \bar{u}, \\ v(0) &= 0, \qquad v(z_i) = 0. \end{aligned} \tag{4.7}$$

The boundary condition on ground level is made non-dimensional by merely changing the dimensional wind speeds by the non-dimensional one as the value of the wind speed is equal to zero.

The boundary condition at the top of the ABL is slightly different. As the height z is made non-dimensional by dividing it by the ABL height, the height of the new upper boundary condition is one. Also, the value of the boundary for wind speed u will no longer be $\bar{u}$ but simply one. This is due to the fact that wind speed u is made non-dimensional by dividing it with the value of the geostrophic wind speed.

New non-dimensional Equations of Motion

Combining the information obtained from Equation (4.3), Equation (4.4), Equation (4.5) and Equation (4.6), the following new non-dimensional equations of motion are obtained

$$\begin{aligned} \frac{\bar{u}^2}{z_i}\hat{w}\hat{u}_{\hat{z}} &= f \cdot \bar{u}\hat{v} + \frac{\bar{u}}{z_i^2}K_M\hat{u}_{\hat{z}\hat{z}}, \\ \frac{\bar{u}^2}{z_i}\hat{w}\hat{v}_{\hat{z}} - f\bar{u} &= -\bar{u}\hat{u}f + \frac{\bar{u}}{z_i^2}K_M\hat{v}_{\hat{z}\hat{z}}. \end{aligned} \tag{4.8}$$

To simplify Equation (4.8), all terms are divided by $f\bar{u}$. The simplification makes solving the system easier, as the wind speed u and v will no longer be multiplied by any parameters. Doing this operation gives Equation (4.9)

$$\begin{aligned} \frac{\bar{u}\hat{w}}{z_i f}\hat{u}_{\hat{z}} &= \hat{v} + \frac{K_M}{f z_i^2}\hat{u}_{\hat{z}\hat{z}}, \\ \frac{\bar{u}\hat{w}}{z_i f}\hat{v}_{\hat{z}} - 1 &= -\hat{u} + \frac{K_M}{f z_i^2}\hat{v}_{\hat{z}\hat{z}}. \end{aligned} \tag{4.9}$$

Constants N and W are introduced for the sake of clarity. This will transform Equation (4.9) into Equation (4.10).

$$\begin{aligned} W\hat{u}_{\hat{z}} &= \hat{v} + N\hat{u}_{\hat{z}\hat{z}}, \\ W\hat{v}_{\hat{z}} - 1 &= -\hat{u} + N\hat{v}_{\hat{z}\hat{z}}, \end{aligned} \tag{4.10}$$

which means that constants N and W will have the following values

$$N = \frac{K_M}{f z_i^2}, \qquad W = \frac{\bar{u}\hat{w}}{z_i f}. \tag{4.11}$$

Subsequently, using the values of parameters discussed in Section 2.6

$$N = \frac{5}{1.1 \cdot 10^{-4} \cdot 1000^2} \approx 4.5 \cdot 10^{-2}, \qquad W = \frac{10 \cdot 0.0025}{1000 \cdot 1.1 \cdot 10^{-4}} \approx 2.3 \cdot 10^{-1}. \tag{4.12}$$

The following section will focus on solving these equations of motion.

4.3. Solving Modified Linear Ekman Spiral

To solve the system found in Section 4.2, the focus is first put on solving for wind speed v. Thereafter, the system is solved for wind speed u. This technique of solving the coupled system is similar to what was done to solve the classical Ekman spiral, discussed in Section 3.2.

The coupled system of differential equations given in Equation (4.10) is rewritten, so that an ordinary differential equation for wind speed v is obtained. This is done via taking the second equation in the system and rewriting it to the following

$$\hat{u}(\hat{z}) = 1 - W\hat{v}_{\hat{z}} + N\hat{v}_{\hat{z}\hat{z}}. \tag{4.13}$$

When the derivative with respect to the height is taken of Equation (4.13) and substituted into the first equation in the system given in Equation (4.10), an expression is obtained only containing wind speed v. This expression can be seen in Equation (4.14)

$$W^2\hat{v}_{zz} - 2WN\hat{v}_{zzz} + N^2\hat{v}_{zzzz} = -\hat{v}. \tag{4.14}$$

As this is an ordinary differential equation, it can be solved for wind speed v. To derive the solution of the above mentioned equation, it is assumed that the solution $\hat{v}(\hat{z})$ will be of the following form

$$\hat{v}(\hat{z}) = \mathrm{e}^{\xi\hat{z}}. \tag{4.15}$$

Substituting Equation (4.15) into Equation (4.14), will give rise to the next steps in solving the differential equation

$$\begin{aligned} \mathrm{e}^{\xi\hat{z}}\left(W^2\xi^2 - 2WN\xi^3 + N^2\xi^4\right) &= \mathrm{e}^{\xi\hat{z}}, \\ \mathrm{e}^{\xi\hat{z}}\left(W^2\xi^2 - 2WN\xi^3 + N^2\xi^4 - 1\right) &= 0, \\ \left(W\xi - N\xi^2\right)^2 &= -1, \\ N\xi^2 - W\xi &= \pm i. \end{aligned} \tag{4.16}$$

In these steps, it is used that the exponential function will never equal 0. Note that the above Equation (4.16) is a regular second degree polynomial in ξ

$$\begin{aligned} \xi &= \frac{W}{2N} \pm \frac{1}{2N}\sqrt{W^2 \pm 4Ni}, \\ \left(\xi - \frac{W}{2N}\right)^2 &= \frac{1}{4N^2}\left(W^2 \pm 4Ni\right), \\ &= \frac{W^2}{4N^2} \pm \frac{i}{N}. \end{aligned} \tag{4.17}$$

Taking the square root of the right hand side of Equation (4.17) will not be done. Instead, a different strategy is used. It is a complex number, hence it will be rewritten using the polar form

$$z = r(\cos\hat{\theta} + i\sin\hat{\theta}) = re^{i\hat{\theta}}. \tag{4.18}$$

Here, $z = a + bi$ with $a, b \in \mathbb{R}$ is a complex number, unequal to 0. Then also, $r = \sqrt{a^2 + b^2}$ is the modulus of this complex number and $\hat{\theta}$ an argument of this complex number. For the cosine and sine it will hold that $\cos\hat{\theta} = \frac{a}{r}$ and $\sin\hat{\theta} = \frac{b}{r}$. As the cosine and sine are both periodic in 2π, there are infinitely many options for $\hat{\theta}$. The principal value of this argument is defined as θ.

The complex number that needs to be rewritten has values for a and b, which are specified in (4.19)

$$\begin{aligned} a &= \frac{W^2}{4N^2}, \\ b &= \frac{1}{N}. \end{aligned} \tag{4.19}$$

Note that both values are positive. Therefore, the modulus, cosine and sine can be determined. These can be seen in Equation (4.20)

$$\begin{aligned} r = \sqrt{a^2 + b^2} &= \sqrt{\left(\frac{W^2}{4N^2}\right)^2 + \left(\frac{1}{N}\right)^2} = \sqrt{\frac{W^4 + 16N^2}{16N^4}} = \frac{\sqrt{W^4 + 16N^2}}{4N^2}, \\ \cos\theta = \frac{a}{r} &= \frac{\frac{W^2}{4N^2}}{\frac{\sqrt{W^4+16N^2}}{4N^2}} = \frac{W^2}{\sqrt{W^4 + 16N^2}}, \\ \sin\theta = \frac{b}{r} &= \frac{\frac{1}{N}}{\frac{\sqrt{W^4+16N^2}}{4N^2}} = \frac{4N}{\sqrt{W^4 + 16N^2}}. \end{aligned} \tag{4.20}$$

This information is substituted back into Equation (4.17)

$$\begin{aligned} \left(\xi - \frac{W}{2N}\right)^2 &= re^{i\theta}, \\ \xi - \frac{W}{2N} &= \pm\sqrt{r}e^{\pm\frac{i\theta}{2}}, \\ \xi &= \frac{W}{2N} \pm \sqrt{r}e^{\pm\frac{i\theta}{2}}. \end{aligned} \tag{4.21}$$

Solutions were assumed to be of a specific form, which can be found in Equation (4.15). A short inspection of the exponent is made of these solutions

$$\begin{aligned} \xi\hat{z} &= \left(\frac{W}{2N} \pm \sqrt{r}e^{\pm\frac{i\theta}{2}}\right)\hat{z}, \\ &= \frac{W}{2N}\hat{z} \pm \sqrt{r}\hat{z}\left(\cos\left(\pm\frac{\theta}{2}\right) + i\sin\left(\pm\frac{\theta}{2}\right)\right), \\ &= \frac{W}{2N}\hat{z} \pm \sqrt{r}\hat{z}\left(\cos\left(\frac{\theta}{2}\right) \pm i\sin\left(\frac{\theta}{2}\right)\right). \end{aligned} \tag{4.22}$$

Now, the solution of the differential equation shown in Equation (4.14), will be a combination of these solutions. Having all these expressions for ξ, they can be combined to derive an expression for the wind speed $\hat{v}(\hat{z})$, which can be seen in Equation (4.23)

$$\begin{aligned}\hat{v}(\hat{z}) = a_1 \mathrm{e}^{\left(\frac{W}{2N}+\sqrt{r}\cos\left(\frac{\theta}{2}\right)\right)\hat{z}} \mathrm{e}^{i\sqrt{r}\hat{z}\sin\left(\frac{\theta}{2}\right)} + a_2 \mathrm{e}^{\left(\frac{W}{2N}+\sqrt{r}\cos\left(\frac{\theta}{2}\right)\right)\hat{z}} \mathrm{e}^{-i\sqrt{r}\hat{z}\sin\left(\frac{\theta}{2}\right)} \\ + a_3 \mathrm{e}^{\left(\frac{W}{2N}-\sqrt{r}\cos\left(\frac{\theta}{2}\right)\right)\hat{z}} \mathrm{e}^{i\sqrt{r}\hat{z}\sin\left(\frac{\theta}{2}\right)} + a_4 \mathrm{e}^{\left(\frac{W}{2N}-\sqrt{r}\cos\left(\frac{\theta}{2}\right)\right)\hat{z}} \mathrm{e}^{-i\sqrt{r}\hat{z}\sin\left(\frac{\theta}{2}\right)}.\end{aligned} \tag{4.23}$$

Equation (4.23) is studied further in Equation (4.24)

$$\begin{aligned}\hat{v}(\hat{z}) &= a_1 \mathrm{e}^{\left(\frac{W}{2N}+\sqrt{r}\cos\left(\frac{\theta}{2}\right)\right)\hat{z}} \left(\cos\left(\sqrt{r}\hat{z}\sin\left(\frac{\theta}{2}\right)\right) + i\sin\left(\sqrt{r}\hat{z}\sin\left(\frac{\theta}{2}\right)\right)\right) \\ &+ a_2 \mathrm{e}^{\left(\frac{W}{2N}+\sqrt{r}\cos\left(\frac{\theta}{2}\right)\right)\hat{z}} \left(\cos\left(-\sqrt{r}\hat{z}\sin\left(\frac{\theta}{2}\right)\right) + i\sin\left(-\sqrt{r}\hat{z}\sin\left(\frac{\theta}{2}\right)\right)\right) \\ &+ a_3 \mathrm{e}^{\left(\frac{W}{2N}-\sqrt{r}\cos\left(\frac{\theta}{2}\right)\right)\hat{z}} \left(\cos\left(\sqrt{r}\hat{z}\sin\left(\frac{\theta}{2}\right)\right) + i\sin\left(\sqrt{r}\hat{z}\sin\left(\frac{\theta}{2}\right)\right)\right) \\ &+ a_4 \mathrm{e}^{\left(\frac{W}{2N}-\sqrt{r}\cos\left(\frac{\theta}{2}\right)\right)\hat{z}} \left(\cos\left(-\sqrt{r}\hat{z}\sin\left(\frac{\theta}{2}\right)\right) + i\sin\left(-\sqrt{r}\hat{z}\sin\left(\frac{\theta}{2}\right)\right)\right), \\ &= (a_1+a_2)\,\mathrm{e}^{\left(\frac{W}{2N}+\sqrt{r}\cos\left(\frac{\theta}{2}\right)\right)\hat{z}} \cos\left(\sqrt{r}\hat{z}\sin\left(\frac{\theta}{2}\right)\right) + (a_1-a_2)\,\mathrm{e}^{\left(\frac{W}{2N}+\sqrt{r}\cos\left(\frac{\theta}{2}\right)\right)\hat{z}} i\sin\left(\sqrt{r}\hat{z}\sin\left(\frac{\theta}{2}\right)\right) \\ &+ (a_3+a_4)\,\mathrm{e}^{\left(\frac{W}{2N}-\sqrt{r}\cos\left(\frac{\theta}{2}\right)\right)\hat{z}} \cos\left(\sqrt{r}\hat{z}(\sin\left(\frac{\theta}{2}\right)\right) + (a_3-a_4)\,\mathrm{e}^{\left(\frac{W}{2N}-\sqrt{r}\cos\left(\frac{\theta}{2}\right)\right)\hat{z}} i\sin\left(\sqrt{r}\hat{z}\sin\left(\frac{\theta}{2}\right)\right).\end{aligned} \tag{4.24}$$

Hence, in total

$$\begin{aligned}\hat{v}(\hat{z}) = b_1 \mathrm{e}^{\left(\frac{W}{2N}+\sqrt{r}\cos\left(\frac{\theta}{2}\right)\right)\hat{z}} \cos\left(\sqrt{r}\hat{z}\sin\left(\frac{\theta}{2}\right)\right) + b_2 \mathrm{e}^{\left(\frac{W}{2N}+\sqrt{r}\cos\left(\frac{\theta}{2}\right)\right)\hat{z}} \sin\left(\sqrt{r}\hat{z}\sin\left(\frac{\theta}{2}\right)\right) \\ + b_3 \mathrm{e}^{\left(\frac{W}{2N}-\sqrt{r}\cos\left(\frac{\theta}{2}\right)\right)\hat{z}} \cos\left(\sqrt{r}\hat{z}\sin\left(\frac{\theta}{2}\right)\right) + b_4 \mathrm{e}^{\left(\frac{W}{2N}-\sqrt{r}\cos\left(\frac{\theta}{2}\right)\right)\hat{z}} \cos\left(\sqrt{r}\hat{z}\cos\left(\frac{\theta}{2}\right)\right).\end{aligned} \tag{4.25}$$

The above solution for wind speed v is not manageable and will be simplified by introducing three different constants p, k and q. These constants are defined below

$$p = \frac{W}{2N} + \sqrt{r}\cos\left(\frac{\theta}{2}\right), \qquad k = \frac{W}{2N} - \sqrt{r}\cos\left(\frac{\theta}{2}\right), \qquad q = \sin\left(\sqrt{r}\frac{\theta}{2}\right). \tag{4.26}$$

Using the constants defined in Equation (4.26) transforms the solution for wind speed v given in Equation (4.25) into

$$\hat{v}(\hat{z}) = \mathrm{e}^{p\hat{z}}\left(b_1\cos\left(q\hat{z}\right) + b_2\sin\left(q\hat{z}\right)\right) + \mathrm{e}^{k\hat{z}}\left(b_3\cos\left(q\hat{z}\right) + b_4\sin\left(q\hat{z}\right)\right). \tag{4.27}$$

Note that, same as with the classical Ekman spiral, the above solution for wind speed v has four unknown constants which need to be determined using the boundary conditions. This will be done in the following section.

4.3.1. Boundary conditions for Specific Wind Speed

There are four constants, and thus there should be four boundary conditions imposed on the system. Generally, the boundary conditions were discussed in Section 2.5. These were made non-dimensional in Section 4.2 and will now be rewritten for wind speed v.

Two of the four imposed boundary conditions are not related to wind speed v, but instead to wind speed u. Hence, these boundary conditions will be rewritten, as to be related to wind speed v. This is done using the second equation of the coupled system of differential equations given in Equation (4.10). In this differential equation, first the value of the boundary condition at ground level is substituted

$$W\hat{v}_{\hat{z}}(0) - 1 = -\hat{u}(0) + N\hat{v}_{\hat{z}\hat{z}}(0). \tag{4.28}$$

It directly follows that

$$W\hat{v}_{\hat{z}}(0) - N\hat{v}_{\hat{z}\hat{z}}(0) = 1. \tag{4.29}$$

For the boundary condition at the top of the ABL height, the same steps are taken. The substitution can be seen in Equation (4.30)

$$W\hat{v}_{\hat{z}}(1) - 1 = -\hat{u}(1) + N\hat{v}_{\hat{z}\hat{z}}(1), \tag{4.30}$$

hence the next boundary conditions will be

$$W\hat{v}_{\hat{z}}(1) = N\hat{v}_{\hat{z}\hat{z}}(1). \tag{4.31}$$

Thus, in total the four boundary conditions that are imposed on wind speed v are the following

$$\begin{aligned} \hat{v}(0) = 0, \qquad & \hat{v}(1) = 0, \\ W\hat{v}_{\hat{z}}(0) - N\hat{v}_{\hat{z}\hat{z}}(0) = 1, \qquad & W\hat{v}_{\hat{z}}(1) = N\hat{v}_{\hat{z}\hat{z}}(1). \end{aligned} \tag{4.32}$$

If one solves the system for wind speed u, the boundary conditions can be rewritten to four conditions which relate to wind speed u in a similar manner.

4.3.2. Determining Constants in Solution for Wind Speed

In Section 4.3.1, four boundary conditions for wind speed v which can be used to determine the values of the constants of the solution given in Equation (4.27), were determined.

To use the last two boundary conditions given in Equation (4.3.1), the derivative of wind speed v with respect to the height needs to be determined. The first derivative of the wind speed with respect to the height is given in Equation (4.33)

$$\begin{aligned} \hat{v}_{\hat{z}}(\hat{z}) = p\mathrm{e}^{p\hat{z}} \left(b_1 \cos(q\hat{z}) + b_2 \sin(q\hat{z})\right) + \mathrm{e}^{p\hat{z}} \left(-qb_1 \sin(q\hat{z}) + b_2 q \cos(q\hat{z})\right) \\ + k\mathrm{e}^{k\hat{z}} \left(b_3 \cos(q\hat{z}) + b_4 \sin(q\hat{z})\right) + \mathrm{e}^{k\hat{z}} \left(-qb_3 \sin(q\hat{z}) + b_4 \cos(q\hat{z})\right). \end{aligned} \tag{4.33}$$

Also, the second derivative of the wind speed with respect to the height is needed. This derivative is given in Equation (4.34)

$$\begin{aligned} \hat{v}_{\hat{z}\hat{z}}(\hat{z}) = p^2\mathrm{e}^{p\hat{z}} \left(b_1 \cos(q\hat{z}) + b_2 \sin(q\hat{z})\right) + 2p\mathrm{e}^{p\hat{z}} \left(-qb_1 \sin(q\hat{z}) + b_2 q \cos(q\hat{z})\right) \\ + \mathrm{e}^{pz} \left(-q^2 b_1 \cos(q\hat{z}) - q^2 b_2 \sin(q\hat{z})\right) + k^2\mathrm{e}^{k\hat{z}} \left(b_3 \cos(q\hat{z}) + b_4 \sin(q\hat{z})\right) \\ + 2k\mathrm{e}^{k\hat{z}} \left(-qb_3 \sin(q\hat{z}) + b_4 q \cos(q\hat{z})\right) + \mathrm{e}^{kz} \left(-q^2 b_3 \cos(q\hat{z}) - q^2 b_4 \sin(q\hat{z})\right). \end{aligned} \tag{4.34}$$

The first boundary condition given in Equation (4.3.1) is used. This gives the following

$$b_1 + b_3 = 0, \qquad \Rightarrow \qquad -b_1 = b_3. \tag{4.35}$$

The other boundary conditions will also be used, but not written out. Instead, a matrix representation of the system that needs to be solved to determine the values of the constants can be found in Appendix A.1. The matrix is 3×3, as the condition posed in Equation (4.35) is already implemented into the solution.

Solving the matrix-vector equation gives the values of the constants. The exact values of these constants are not written down in this thesis, as this will take up an entire page. Instead the code used to compute the values of the constants can be found in Appendix A.2. Having computed the values of the constants, the solution for wind speed u can be determined. This will be done in the following section.

4.3.3. Solution for Remaining Wind Speed

The solution for wind speed v has been determined in Section 4.3, and the values of the constants in the solution were discussed in Section 4.3.2. Now, the solution for wind speed u can be determined.

The solution for wind speed u is determined using Equation (4.13). The two derivatives in this

equation can be found in Equation (4.33) and Equation (4.34). Thus,

$$\begin{aligned}\hat{u}(\hat{z}) = 1 &- W\left(p\mathrm{e}^{p\hat{z}}\left(b_1\cos(q\hat{z}) + b_2\sin(q\hat{z})\right) + \mathrm{e}^{p\hat{z}}\left(-qb_1\sin(q\hat{z}) + b_2q\cos(q\hat{z})\right)\right)\\ &- W\left(k\mathrm{e}^{k\hat{z}}\left(b_3\cos(q\hat{z}) + b_4\sin(q\hat{z})\right) + \mathrm{e}^{k\hat{z}}\left(-qb_3\sin(q\hat{z}) + b_4\cos(q\hat{z})\right)\right)\\ &+ N\left(p^2\mathrm{e}^{p\hat{z}}\left(b_1\cos(q\hat{z}) + b_2\sin(q\hat{z})\right) + 2p\mathrm{e}^{p\hat{z}}\left(-qb_1\sin(q\hat{z}) + b_2q\cos(q\hat{z})\right)\right)\\ &+ N\left(\mathrm{e}^{pz}\left(-q^2b_1\cos(q\hat{z}) - q^2b_2\sin(q\hat{z})\right) + k^2\mathrm{e}^{k\hat{z}}\left(b_3\cos(q\hat{z}) + b_4\sin(q\hat{z})\right)\right)\\ &+ N\left(2k\mathrm{e}^{k\hat{z}}\left(-qb_3\sin(q\hat{z}) + b_4q\cos(q\hat{z})\right) + \mathrm{e}^{kz}\left(-q^2b_3\cos(q\hat{z}) - q^2b_4\sin(q\hat{z})\right)\right).\end{aligned} \tag{4.36}$$

Note that both solutions for wind speeds u and v have changed drastically now that the modified linear version of Ekman's spiral is studied. In Section 4.4, both solutions are visualized.

4.4. Visualization of the Modified Linear Ekman Spiral

This section will discuss several hodographs of the solution to the modified linear Ekman spiral. It will also compare the new spiral to the classical Ekman spiral, discussed previously in Section 3.3. Again, the influence of different parameters are discussed.

A hodograph is again made of wind speed v and u, given in Equation (4.27) and Equation (4.36) respectively. The constants in these equations are discussed in Section 4.3.2. The hodograph can be seen in Figure 4.1.

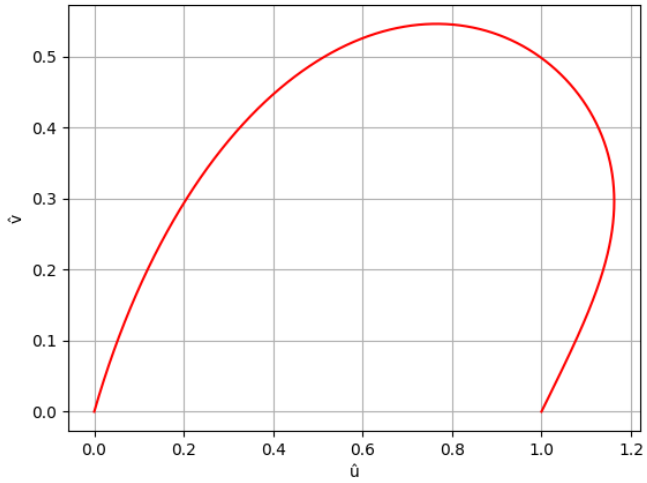

Figure 4.1: The hodograph of the modified linear Ekman spiral with parameter values $N = 4.5 \cdot 10^{-2}$ and $W = 2.3 \cdot 10^{-1}$.

The spiral, which appeared in the hodograph of the classical Ekman spiral in Figure 3.1, is no longer in the hodograph of the modified linear Ekman spiral. This will be discussed later, when analyzing the influence of difference parameters on the modified linear Ekman spiral.

Again, similar to Section 3.3, another hodograph is made with points indicating the height. However, now that the height is non-dimensionalized, the dots do not represent the same heights as before. Now they are fractions of the ABL height. This hodograph can be seen in Figure 4.2.

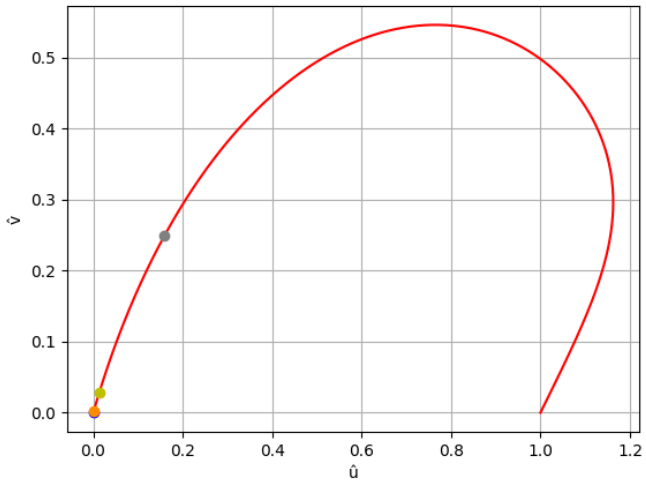

Figure 4.2: A hodograph of the modified linear Ekman spiral with parameter values $N = 4.5 \cdot 10^{-2}$ and $W = 2.3 \cdot 10^{-1}$ with dots indicating certain heights.

The blue dot, which is just beneath the orange dot, is placed at a fraction of $\frac{1}{10000}$ of the ABL height. Next, the orange dot is a fraction of $\frac{1}{1000}$ of the ABL height. The third dot, which is yellow, is placed at $\frac{1}{100}$ of the ABL height. Lastly, the grey dot is placed at $\frac{1}{10}$ of the ABL height.

4.4.1. Comparing Modified Linear Ekman Spiral and Classical Ekman Spiral

The modified linear Ekman spiral and classical Ekman spiral can be compared when taking the vertical wind speed in the modified version equal to 0. By dividing the classical Ekman spiral by the geostrophic wind speed, it is scaled so that it can be compared to the modified version. The wind speeds of the scaled version of the classical Ekman spiral are denoted by u_{n} and v_{n}. The two hodographs are shown in Figure 4.3.

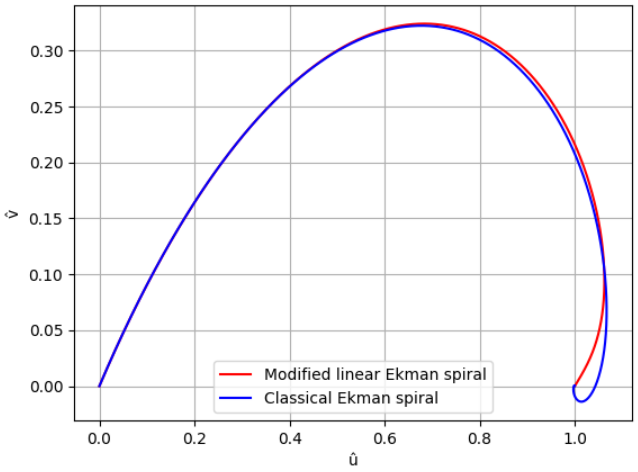

Figure 4.3: Hodograph of the modified linear Ekman spiral in red and hodograph of classical Ekman spiral in blue, parameters equal to $z_i = 1000$, $\bar{u} = 10$ $f = 1.1 \cdot 10^{-4}$, $K_M = 5$ and $\hat{w} = 0$.

In the above figure, the axis are indicated by the non-dimensional wind speeds. The wind speed for the classical Ekman spiral is thus also divided by the geostrophic wind speed.

A difference between the two is clearly visible. This difference can be explained via the chosen height of the ABL. In the classical Ekman spiral, Walfrid Ekman put his boundary at an infinite height. In reality, the height of the ABL is not infinite. To study this difference, the error between the two hodographs is calculated. The error in wind speed u is defined as the following

$$\varepsilon_u = \sum_{i=1}^{10^5} |u_{\mathrm{n}}(\hat{i}) - \hat{u}(\hat{i})|. \tag{4.37}$$

In the above equation, the parameter $\hat{i}$ is defined

$$\hat{i} = \frac{i}{10^5}, \tag{4.38}$$

so that values of both non-dimensionalized wind speeds u of Ekman's spiral are calculated. By subtracting these from each other, the error becomes smaller when the two hodographs have more overlap. The error in wind speed v is defined similarly to the error for wind speed u given in Equation (5.56)

$$\varepsilon_v = \sum_{i=1}^{10^5} |v_{\mathrm{n}}(\hat{i}) - \hat{v}(\hat{i})|. \tag{4.39}$$

Here, the same definition for parameter $\hat{i}$, given in Equation (5.57), is used. Note that the error does not depend on the height at which the hodograph goes towards the endpoint.

Having defined error for both wind speeds, the error is studied for different heights of the parameter z_i, the height of the ABL. The values are given in Table 4.1. In this table, also the difference in values between the current and previous ABL height is given. This difference is denoted by $\Delta\varepsilon_u$ and $\Delta\varepsilon_v$ for the error in wind speed u and v respectively.

Table 4.1: Both errors of wind speed u and v for different ABL heights including the difference in errors.

z_i	ε_u	ε_v	$\Delta\varepsilon_u$	$\Delta\varepsilon_v$
1000	20095.25	16524.62	-	-
2000	10640.19	8334.83	−9455.06	−8189.79
3000	7057.56	5581.76	−3582.63	−2753.07
4000	5255.80	4197.81	−1801.76	−1383.95
5000	4174.49	3363.20	−1084.31	−834.61
6000	3453.61	2803.80	−720.88	−559.40
7000	2938.71	2401.98	−514.90	−401.82
8000	2552.53	2098.88	−386.18	−303.10
9000	2252.16	1861.75	−300.37	−247.13
10000	2011.87	1670.92	−240.29	−190.83

For a more thorough analysis of the correlation between the error and the height of the ABL, a graph is made of the errors. This graph can be seen in Figure 4.4.

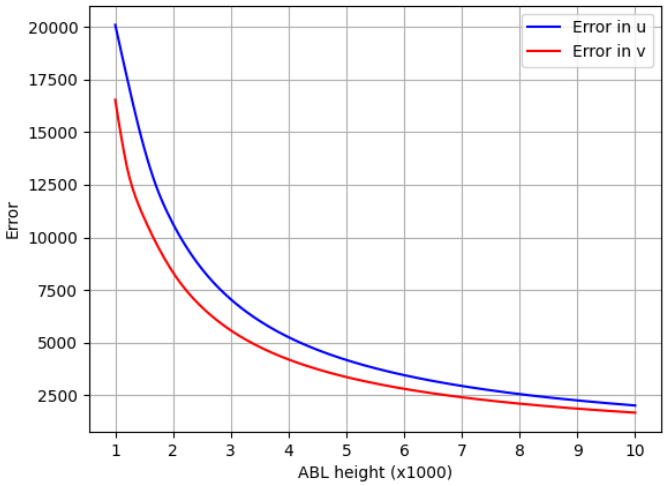

Figure 4.4: The error of both wind speed u and v against the parameter z_i.

The Python code to create Figure 4.4 and the values in Table 4.1 can be found in Appendix B.1. The difference in error in Table 4.1 was computed by hand.

It is clear that the error decreases when the height of the ABL increases. However, a drastic decrease in error happens in the first 4000 metres as opposed to the last 4000 metres. This can be attributed to parameter N being inversely squared proportional to the parameter z_i.

Emeis stated in his book (Emeis, 2018) that the ABL height might be as high as 2500 metres. The error at this height will still be around 6000 for ε_v and 8000 for ε_u, but still less than for an ABL height of 1000 metres. Figure 4.3 will be recreated, but with this different value of z_i. This can be seen in Figure 4.5.

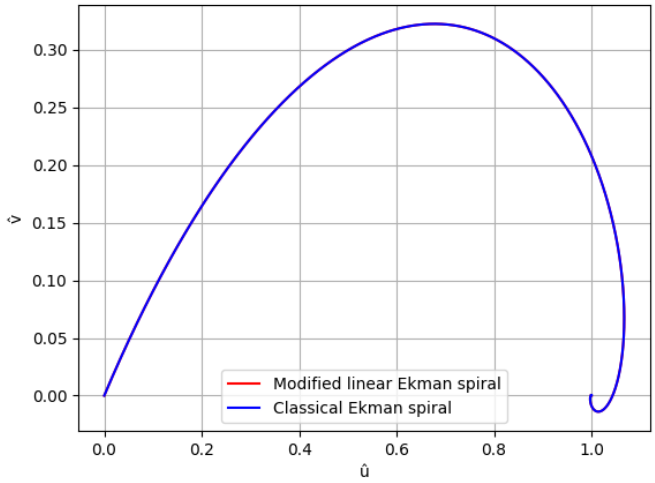

Figure 4.5: Hodograph of modified linear Ekman spiral in red and hodograph of classical Ekman spiral in blue, paramaters equal to $z_i = 2500$, $\bar{u} = 10$, $f = 1.1 \cdot 10^{-4}$, $K_M = 5$ and $\hat{w} = 0$.

From the figure above, in which the red and blue hodographs have merged, there no longer seems to be any difference between the modified linear Ekman spiral and the classical Ekman spiral. However, when calculating the error, it is still equal to $\varepsilon_u = 8498.99$ and $\varepsilon_v = 6682.60$.

For sake of comparison and to study the spiral, the parameter z_i will from now standard be set equal to 2500 metres.

4.4.2. Influence of the Coriolis parameter

First, Figure 4.2 is recreated, using the different value for parameter z_i, as discussed in previous Section 4.4.1. In this figure, the dots remain at the same places as discussed before.

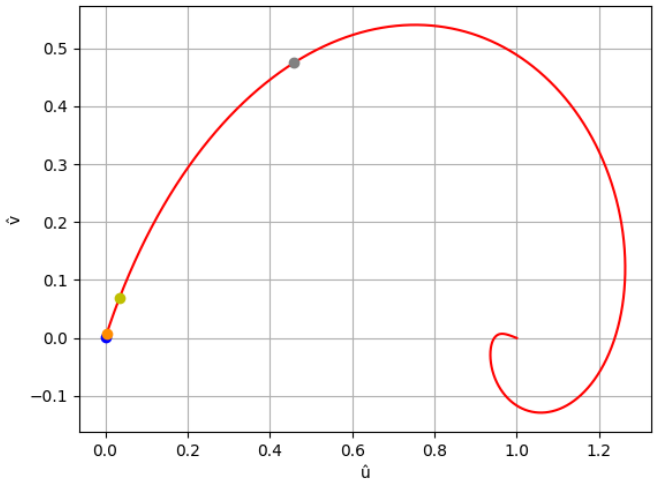

Figure 4.6: Hodograph of the modified linear Ekman spiral with dots indicating certain heights, parameter values $\bar{u} = 10$, $f = 1.1 \cdot 10^{-5}$, $K_M = 5$, $z_i = 2500$ and $\hat{w} = 0.0025$.

In Figure 4.6 a clear spiral can be seen again, as opposed to Figure 4.2. The positioning of the dots, however, is similar.

To study the effect of the Coriolis parameter, two different hodographs are made with different values of Coriolis parameter f. The other parameters will remain the same as in Figure 4.6. The two different hodographs can be seen below.

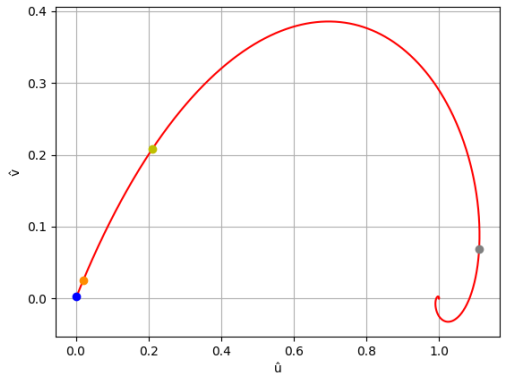

Figure 4.7: A hodograph of the modified linear Ekman Spiral with parameters $\bar{u} = 10$, $f = 1.1 \cdot 10^{-3}$, $K_M = 5$, $z_i = 2500$ and $\hat{w} = 0.0025$.

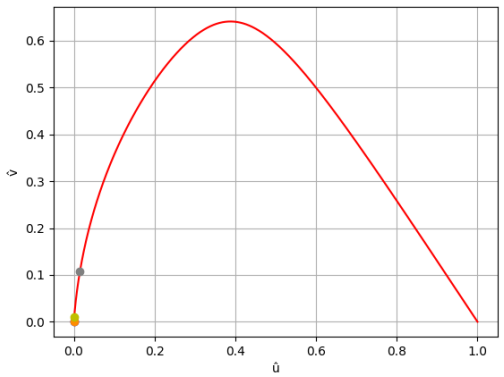

Figure 4.8: A hodograph of the modified linear Ekman Spiral with parameters $\bar{u} = 10$, $f = 1.1 \cdot 10^{-5}$, $K_M = 5$ and $\hat{w} = 0.0025$.

In Figure 4.7 the same effect as for the classical Ekman spiral can be seen; a bigger Coriolis parameter means that the wind speed moves towards the ABL height for a lower height. The opposite holds true for a smaller Coriolis parameter, which can be seen in Figure 4.8.

In both Figures, there is also a difference in the spiral itself. In Figure 4.7, the spiral is shorter. In Figure 4.8, there is no spiral at all.

4.4.3. Influence of the turbulent viscosity

To study the effect of the turbulent viscosity parameter K_M, two different hodographs are made and compared to Figure 4.6.

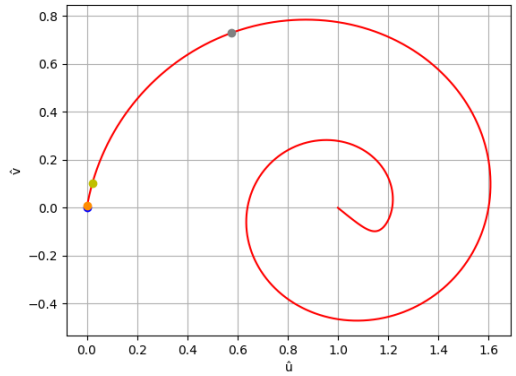

Figure 4.9: A hodograph of the modified linear Ekman Spiral with parameters $\bar{u} = 10$, $f = 1.1 \cdot 10^{-4}$, $K_M = 1$, $z_i = 2500$ and $\hat{w} = 0.0025$.

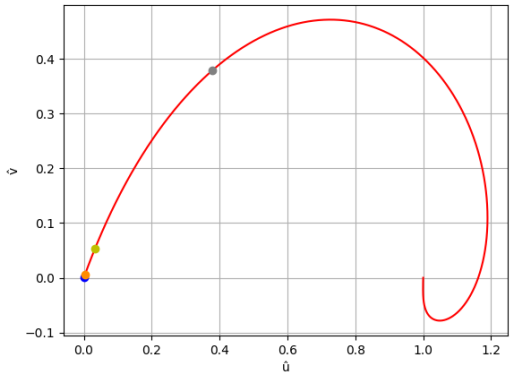

Figure 4.10: A hodograph of the modified linear Ekman Spiral with parameters $\bar{u} = 10$, $f = 1.1 \cdot 10^{-4}$, $K_M = 10$ and $\hat{w} = 0.0025$.

The dots in both Figure 4.9 and Figure 4.10 are roughly in the same position. This is different than what happened with the classical Ekman spiral. The spiral, however, does change. In Figure 4.9 there is a full loop of the spiral. In Figure 4.10, there is a shorter spiral than in Figure 4.6. Also, at the end of the spiral, an almost straight line towards the boundary point $(1, 0)$ is made. This is discussed further in Section 4.5.

4.4.4. Influence of the geostrophic wind speed

Again, hodographs with different values for the parameter $\bar{u}$, indicating the geostrophic wind speed, are made and compared to Figure 4.6.

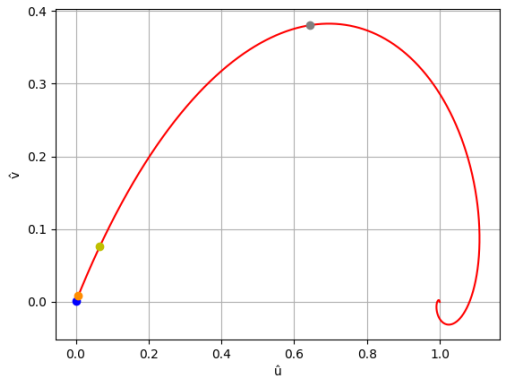

Figure 4.11: A hodograph of the modified linear Ekman Spiral with parameters $\bar{u} = 3$, $f = 1.1 \cdot 10^{-4}$, $K_M = 5$, $z_i = 2500$ and $\hat{w} = 0.0025$.

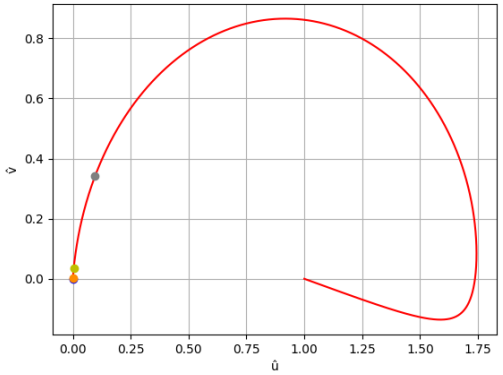

Figure 4.12: A hodograph of the modified linear Ekman Spiral with parameters $\bar{u} = 30$, $f = 1.1 \cdot 10^{-4}$, $K_M = 5$ and $\hat{w} = 0.0025$.

Figure 4.11 seems identical to Figure 4.7, apart from the positioning of the dots. Also, the dots have moved slightly upwards on the spiral. For Figure 4.12, the dots have moved down and there is almost no recognizable spiral left.

The same remark, as was made in Section 4.4.4 about the end of the spiral is still appearing here. The end of the spiral does not follow a spiral shape continuously, but the hodograph rather moves directly towards the end point.

4.4.5. Influence of the ABL height

The parameter z_i, which represents the height of the ABL, is also discussed. Different hodographs are again created for different values of the ABL height.

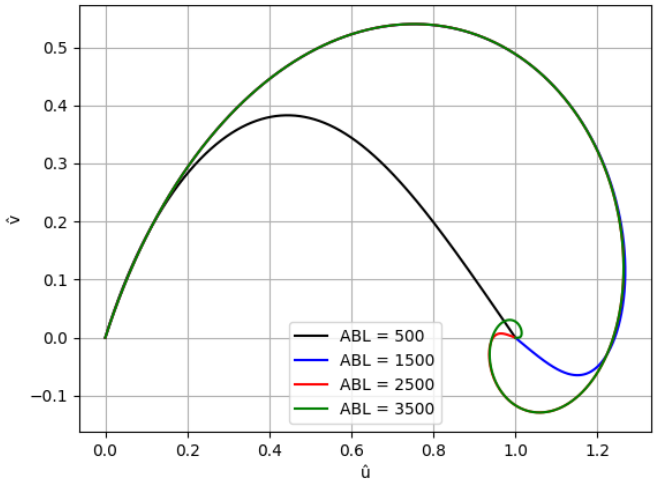

Figure 4.13: Hodgraphs of the modified linear Ekman spiral with parameter values $\bar{u} = 10$, $f = 1.1 \cdot 10^{-4}$, $K_M = 5$, $\hat{w} = 0.0025$ and z_i equal to ABL for the different hodographs.

In Figure 4.13, it can be seen that the hodograph takes a different shape for different heights of the ABL. Looking closely, the red and green hodograph overlap for the most part. Hence, it can be concluded that there is little difference in the influence of the ABL height from 2500 metres or higher.

It should be noted that there are no dots in the above figure, due to the ABL height directly influencing the placement of these dots. This is, because the end point of the hodograph is put at the ABL height.

4.4.6. Influence of the vertical wind speed

The influence of the vertical wind speed is also analyzed via studying the hodograph for different values of parameter $\hat{w}$.

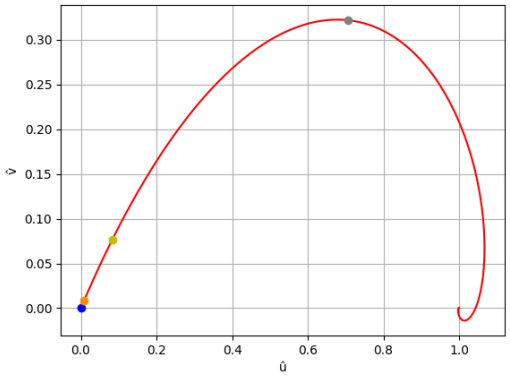

Figure 4.14: A hodograph of the modified linear Ekman Spiral with parameters $\bar{u} = 3$, $f = 1.1 \cdot 10^{-4}$, $K_M = 5$, $z_i = 2500$ and $\hat{w} = 0$.

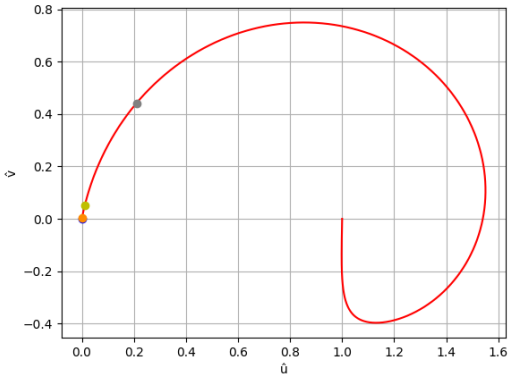

Figure 4.15: A hodograph of the modified linear Ekman Spiral with parameters $\bar{u} = 30$, $f = 1.1 \cdot 10^{-4}$, $K_M = 5$ and $\hat{w} = 0.05$.

By decreasing the vertical wind speed, the hodograph, seen in Figure 4.14 the appearance is similar to that of the classical Ekman spiral. This coincides with what has been discussed in Section 4.4.1. The dots have moved forward slightly. In Figure 4.15, the hodograph with a bigger vertical wind speed can be seen. The dots have moved back and the spiral has taken another form, resembling more the

upper half of a circle.

As the vertical wind speed is the most important parameter, it is studied even more. Hodographs are made with even more different values of $\hat{w}$, which can be seen in Figure 4.16.

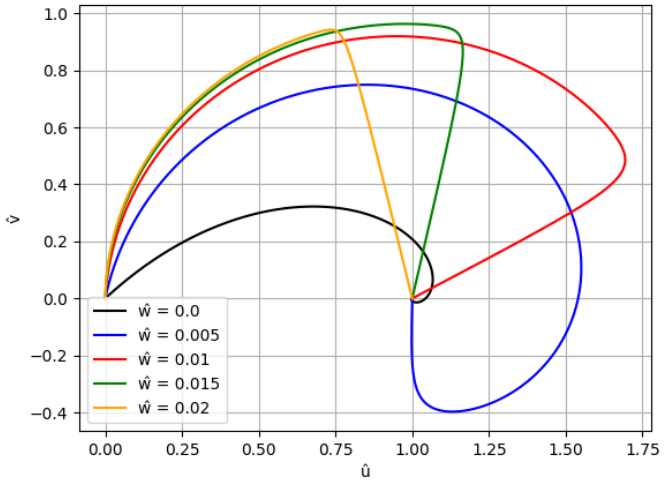

Figure 4.16: Hodograph of the modified linear Ekman spiral with parameters $\bar{u} = 30$, $f = 1.1 \cdot 10^{-4}$, $K_M = 5$ and $\hat{w}$ varies per hodograph ranging from 0 to 0.02.

In the above figure it can be seen that the shape of the hodograph changes drastically for different values of the vertical wind speed. For higher wind speeds, beyond 0.005, no longer any spiral shape can be recognized in the hodograph.

4.4.7. Exaggerating the spiral in the Modified Linear Ekman Spiral

During the process of analyzing several values for the above mentioned parameters, a certain set of parameters amplified the spiral in the hodograph of the modified linear Ekman spiral drastically. This can be seen in Figure 4.17.

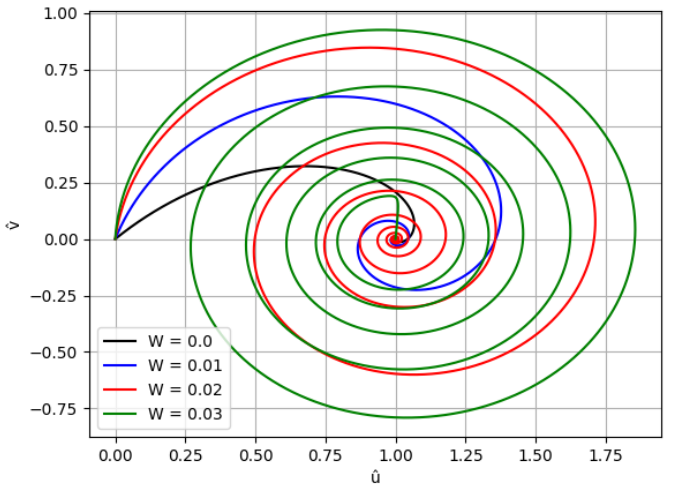

Figure 4.17: Hodograph of modified linear Ekman spiral with parameter values $N = 4.55 \cdot 10^{-5}$ and W is equal to values ranging from 0 to 0.03.

For higher values of parameter W, the spiral seems to loop more around the end point $(1, 0)$. Also, there is a bigger maximum speed for both horizontal wind speeds when parameter W increases. However,

higher values of parameter W are not possible. This is discussed in Section 4.5.

To study the spiral in more detail, a close up of the above hodograph is made around the end point. This can be seen below.

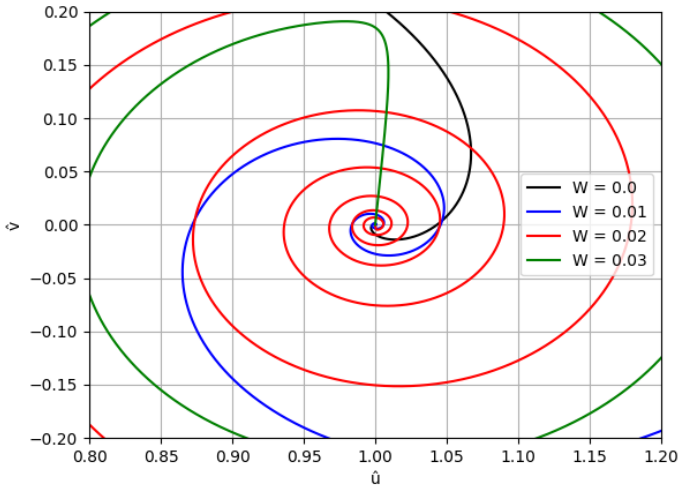

Figure 4.18: A close up of the hodograph of the modified linear Ekman spiral with parameter values $N = 4.55 \cdot 10^{-5}$ and W equal to values ranging from 0 to 0.03.

It can be seen that the hodograph spirals around the end point with values W unequal to 0.03. For this value, the hodograph simply goes in a straight line towards the end point, which could also be seen when discussing the influence of the vertical wind speed, geostrophic wind speed, turbulent viscosity and Coriolis parameter.

4.5. Numerical Remarks Modified Linear Ekman Spiral

There are several important remarks to be made when visualizing the modified linear Ekman spiral using a numerical implementation. These remarks will be discussed in this section.

First, the solution for both wind speeds depends on an exponential which does not have a negative exponent. Hence, it will tend to large values if the exponent gets too large. This can happen when changing parameters in the solution to study different scenarios. The following exponential influences the wind speed

$$e^p = e^{\frac{W}{2N} + \sqrt{r}\cos\left(\frac{\theta}{2}\right)}. \tag{4.40}$$

Note that in Equation (4.40), the cosine remains between -1 and 1 and the parameter $\sqrt{r}$ is of lower order than $\frac{W}{2N}$. The value of $\frac{W}{2N}$ might be very large, due to N being small. This is why in Section 4.4.7, the hodograph could not be plotted for higher W values.

The second remark has to do with the behaviour of the spiral towards the end point $(1, 0)$. In some figures, see Figure 4.10, Figure 4.12 and Figure 4.15, the spiral moves in an almost straight line at the end. It is thought that this happens due to not enough grid points existing around the end point. However, if one defines a grid which takes steps of order $1 \cdot 10^{-9}$ at the last 0.05 height, Figure 4.19 is obtained.

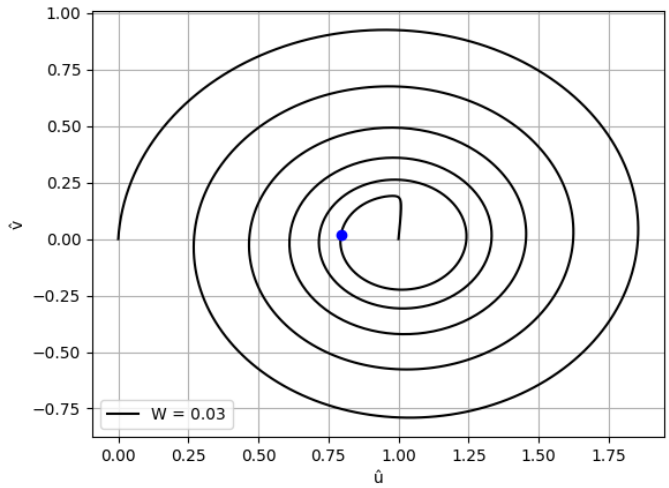

Figure 4.19: Hodograph of modified linear Ekman spiral with parameter values $N = 4.55 \cdot 10^{-5}$ and $W = 0.03$, with non-equidistant grid.

In the figure above, the blue dot represents from where the gridpoints have decreased to taking a step of $1 \cdot 10^{-9}$. The straight line towards the end point thus does not happen due to a non optimal placed grid. This effect could be attributed to the low ABL height. If the ABL would be placed at a greater height, the spiral could spiral more around the end point before ending in it. However, this could not be implemented due to the first numerical remark.

The Python code used to create the figures in this chapter, except the ones concerning the errors between the modified linear Ekman spiral and the classical Ekman spiral, can be found in Appendix D.

4.6. Conclusion on Analysis of Modified Linear Ekman Spiral

This section will conclude on the modified linear Ekman spiral. A short overview of the assumptions, boundary conditions, influence of different parameters and numerical remarks is given.

The assumptions made for the modified linear Ekman spiral are not major. There is assumed to be no gravitational force and no vertical component of the Coriolis force. The first assumption will not influence the hodograph significantly, as it is merely a constant which is subtracted in the vertical wind direction. The assumption that there is no vertical component of the Coriolis force does influence the solution significantly, as allowing a vertical component of the Coriolis force will make the equations of motion, given in Equation (4.1), non-linear.

The boundary conditions imposed on the modified linear Ekman spiral are heavily influenced by the ABL height. These boundary conditions are more realistic than the boundary conditions imposed on the classical Ekman spiral.

Next, the parameters of the modified linear Ekman spiral are discussed. Similar to the classical Ekman spiral, a larger Coriolis parameter influences at which height the wind goes towards the end point. This effect does not appear with the turbulent viscosity parameter. For a smaller geostrophic wind speed or vertical wind speed, the hodograph also moves towards the end point for a lower height. For a larger Coriolis parameter, vertical wind speed or ABL height, a more spiral-like shape can be seen in the hodograph. The same holds for a smaller geostrophic wind speed or turbulent viscosity parameter.

When implementing the modified linear Ekman spiral, there are numerical remarks. The exponential terms in the solution can become too big for a computer to handle, which influences for which parameters the hodograph can be visualized.

In conclusion, the modified linear Ekman spiral is a realistic model for the wind flow. By non-dimensionalizing, an efficient way of relating the spiral to the ABL height is created, which creates a valid way of imposing the boundary conditions. The assumption of no vertical Coriolis force makes the equations of motion easily solvable, as the equations of motion remain linear. All constants can be combined into two parameters, which have an effect on the shape and size of the hodograph. The

major shortcoming lies in the numerical implementation, as due to an exponential term in the solution for both wind speeds, the solution might become too large to visualize a hodograph.

5

Ekman Spiral with Vertical Wind Speed

In this chapter, focus is put on a modified non-linear Ekman spiral. The modified non-linear Ekman spiral will be introduced in Section 5.1. Then, for the sake of simplicity, the equations of motion obtained in Section 5.1 will be non-dimensionalized in Section 5.2. Thereafter, an algorithm to solve the the non-dimensional equations of motion analytically is given in Section 5.3. In Section 5.4, the numerical scheme used in this thesis to determine the non-linear hodograph is given, whereas in Section 5.5 the visualizations of different hodographs is given. In this section, also the influence of the different parameteres in the solutions for the wind speeds is discussed.

5.1. Ekman Spiral with Vertical Wind Speed Ekman Spiral

As already stated before, in Ekman's original paper (Ekman, 1905), the assumption was made that there was no vertical wind speed. Chapter 4 allowed vertical wind speed, but no vertical Coriolis force component. However, in reality there will be such a component. This will change previous discussed equations of motion given in Equation (3.1) into the Equation (5.1). This equation is obtained by taking Equation (2.5) and substituting the Coriolis parameters given in Equation (3.3) and Equation (3.4), both discussed in Chapter 3

$$\begin{aligned} w \cdot u_z + P_x &= vf - w\hat{f} \sin\beta + K_M u_{zz}, \\ w \cdot v_z + P_y &= w\hat{f} \cos\beta - uf + K_M v_{zz}. \end{aligned} \tag{5.1}$$

Note that there is again no equation concerning the vertical wind speed. This is due to the fact that the vertical wind speed is assumed constant, as this reduces the amount of equations in Equation (5.1) from three to two equations. In reality this vertical wind speed varies in height.

5.2. Non-dimensionalization

This section will focus on making the equations of motion given in Equation (5.1) non-dimensional.

Via the same argument given in Chapter 3, the pressure gradient divided by the air density with derivative taken with respect to either x or y will remain constant with height. Therefore, values given in Equation (3.7) will be substituted into the above Equation (5.1).

$$\begin{aligned} w \cdot u_z &= vf - w\hat{f} \sin\beta + K_M u_{zz}, \\ w \cdot v_z - f\bar{u} &= w\hat{f} \cos\beta - uf + K_M v_{zz}. \end{aligned} \tag{5.2}$$

The above mentioned equation will now be non-dimensionalized. This will be done via the same steps taken in Chapter 4. Combining the information obtained from Equation (4.3), Equation (4.4), Equation (4.5) and Equation (4.6), the following new non-dimensional equations of motion are obtained.

$$\begin{aligned} \frac{\bar{u}^2}{z_i} \hat{w} \cdot \hat{u}_{\hat{z}} &= f \cdot \bar{u}\hat{v} - \hat{w}\bar{u}\hat{f} \sin\beta + \frac{\bar{u}}{z_i^2} K_M \hat{u}_{\hat{z}\hat{z}}, \\ \frac{\bar{u}^2}{z_i} \hat{w} \cdot \hat{v}_{\hat{z}} - f\bar{u} &= \bar{u}\hat{w}\hat{f} \cos\beta - \bar{u}\hat{u}f + \frac{\bar{u}}{z_i^2} K_M \hat{v}_{\hat{z}\hat{z}}. \end{aligned} \tag{5.3}$$

To simplify Equation (5.3), all terms are divided by $f\bar{u}$. This gives Equation (5.4)

$$\begin{aligned} \frac{\bar{u}\hat{w}}{z_i f}\cdot\hat{u}_{\hat{z}} &= \hat{v} - \frac{\hat{w}\hat{f}}{f}\sin\beta + \frac{K_M}{f z_i^2}\hat{u}_{\hat{z}\hat{z}}, \\ \frac{\bar{u}\hat{w}}{z_i f}\hat{w}\cdot\hat{v}_{\hat{z}} - 1 &= \frac{\hat{w}\hat{f}}{f}\cos\beta - \hat{u} + \frac{K_M}{f z_i^2}\hat{v}_{\hat{z}\hat{z}}. \end{aligned} \tag{5.4}$$

Constants N, W and F are introduced for the sake of clarity. This will transform Equation (5.4) into Equation (5.5)

$$\begin{aligned} W\cdot\hat{u}_{\hat{z}} &= \hat{v} - F\sin\beta + N\hat{u}_{\hat{z}\hat{z}}, \\ W\cdot\hat{v}_{\hat{z}} - 1 &= F\cos\beta - \hat{u} + N\hat{v}_{\hat{z}\hat{z}}, \end{aligned} \tag{5.5}$$

so constants N, W and F will have the following values

$$N = \frac{K_M}{f z_i^2}, \qquad W = \frac{\bar{u}\hat{w}}{z_i f}, \qquad F = \frac{\hat{w}\hat{f}}{f}. \tag{5.6}$$

Now, using the values of the parameters as discussed in Section 2.6

$$\begin{aligned} N = \frac{5}{1.1\cdot 10^{-4}\cdot 1000^2} \approx 4.5\cdot 10^{-2}, \qquad W = \frac{10\cdot 0.0025}{1000\cdot 1.1\cdot 10^{-4}} \approx 2.3\cdot 10^{-1}, \\ F = \frac{0.0025\cdot 0.90\cdot 10^{-4}}{1.1\cdot 10^{-4}} \approx 2.0\cdot 10^{-3}. \end{aligned} \tag{5.7}$$

Also, it is known that the values for the non-dimensional wind speed u and v are between 0 and 1. The non-dimensional height also lies in this range.

Before continuing on, the sine and cosine in the coupled system of differential equations given in Equation 5.5 are studied. In Section 2.4 it was noted that β was equal to the arc-tangent of the fraction $\frac{v}{u}$. Hence, the sine and cosine of β will equal

$$\sin\beta = \frac{\frac{v}{u}}{\sqrt{1+\left(\frac{v}{u}\right)^2}}, \qquad \cos\beta = \frac{1}{\sqrt{1+\left(\frac{v}{u}\right)^2}} \tag{5.8}$$

Next, an algorithm for solving Equation (5.5) analytically is given in Section 5.3.

5.3. Algorithm Modified Non-linear Ekman Spiral

Due to the non-linear property of the equations of motion, given in Equation (5.5), the system becomes very hard to solve via the same steps taken before in Section 4.3. Therefore, a regular perturbation method, RPM, is used.

First, the problem is generalized. Both equations in the system of equations, given in Equation (5.5), are rewritten to the following general form

$$L^v(\mathbf{x}) = \hat{f}N^v(\mathbf{x}), \tag{5.9}$$

$$L^u(\mathbf{x}) = 1 + \hat{f}N^u(\mathbf{x}). \tag{5.10}$$

Here, the vector $\mathbf{x}$ is the vector consisting of components x_1 and x_2. The superscript, either v or u represents the first and second differential equation in Equation (5.5) respectively.

In Equation (5.9), L^v represent the linear differential operator given by

$$L^v(\mathbf{x}) = -W\cdot\frac{\mathrm{d}}{\mathrm{d}\hat{z}}x_1 + x_2 + N\frac{\mathrm{d}^2}{\mathrm{d}\hat{z}^2}x_1. \tag{5.11}$$

In the same equation, N^v represents the non-linear operator

$$N^v(\mathbf{x}) = \frac{\frac{x_2}{x_1}}{\sqrt{1+\left(\frac{x_2}{x_1}\right)^2}}. \tag{5.12}$$

Next, in Equation (5.10), L^u represent the linear differential operator given by

$$L^u(\mathbf{x}) = W \cdot \frac{\mathrm{d}}{\mathrm{d}\hat{z}} x_2 + x_1 - N \frac{\mathrm{d}^2}{\mathrm{d}\hat{z}^2} x_2. \tag{5.13}$$

In the same equation, N^u represents the non-linear operator

$$N^u(\mathbf{x}) = \frac{1}{\sqrt{1 + \left(\frac{x_2}{x_1}\right)^2}}. \tag{5.14}$$

In the case of the Ekman spiral, the vector $\mathbf{x}$ will consist of wind speed $\hat{u}$ and $\hat{v}$. When using a RPM, these variables are assumed to be of the following form

$$\begin{aligned} \hat{u} &= \sum_{n=0} \hat{u}^n \hat{f}^n \\ \hat{v} &= \sum_{n=0} \hat{v}^n \hat{f}^n \end{aligned} \tag{5.15}$$

Now, each order of $\hat{f}$ is treated separately, starting with $\mathcal{O}(1)$. This will be done in Section 5.3.1. After that, higher orders of $\hat{f}$ are treated.

5.3.1. Order $\mathcal{O}(1)$

In the problem of order $\mathcal{O}(1)$, it is assumed that wind speed u and v both are equal to only the first term of the summation given in Equation (5.15). In other words, it is assumed that $\hat{f}$ equals zero. So, the horizontal wind speeds will be

$$\hat{u} = \hat{u}^0, \qquad \hat{v} = \hat{v}^0. \tag{5.16}$$

Thus, vector $\mathbf{x}$ on which both linear and non-linear operators act, can now be replaced with both wind speeds given in Equation (5.16).

Solving the equations given in Equation (5.9) and Equation (5.9) only requires studying the linear operators, as the non-linear operators drop out due to $\hat{f}$ being equal to 0. First, the linear operator with superscript v, given in Equation (5.11), is studied

$$L^v\left(\begin{pmatrix}\hat{u}^0 \\ \hat{v}^0\end{pmatrix}\right) = -W\hat{u}^0_{\hat{z}} + \hat{v}^0 + N\hat{u}^0_{\hat{z}\hat{z}}. \tag{5.17}$$

Next, the linear operator with superscript u is analyzed

$$L^u\left(\begin{pmatrix}\hat{u}^0 \\ \hat{v}^0\end{pmatrix}\right) = W\hat{v}^0_{\hat{z}} + \hat{u}^0 - N\hat{v}^0_{\hat{z}\hat{z}}. \tag{5.18}$$

Hence, the system of differential equations that needs to be solved is the following

$$\begin{aligned} -W\hat{u}^0_{\hat{z}} + \hat{v}^0 + N\hat{u}^0_{\hat{z}\hat{z}} &= 0, \\ W\hat{v}^0_{\hat{z}} + \hat{u}^0 - N\hat{v}^0_{\hat{z}\hat{z}} &= 1. \end{aligned} \tag{5.19}$$

The system of differential equations given in Equation (5.19) is identical to the system of differential equations for the modified linear Ekman spiral. This system has been solved in Chapter 4. Hence, $\hat{u}^0$ and $\hat{v}^0$ are hereby known solutions to the above system.

5.3.2. Order $\mathcal{O}(\hat{f})$

For the step in the perturbation method, the next order of the problem is studied. The next order means that all terms containing $\mathcal{O}\left(\hat{f}^2\right)$ will be considered equal to 0. Therefore, the new horizontal wind speeds that will be discussed are

$$\hat{v} = \hat{v}^0 + \hat{f}\hat{v}^1, \qquad \hat{u} = \hat{u}^0 + \hat{f}\hat{u}^1. \tag{5.20}$$

Similar steps as in Section 5.3.1 are taken, only now the non-linear operators are studied as well. First, both the linear and non-linear operator with superscript v are discussed. First, the linear operator

$$L^v\left(\begin{pmatrix}\hat{u}^0+\hat{f}\hat{u}^1\\ \hat{v}^0+\hat{f}\hat{v}^1\end{pmatrix}\right)=L^v\left(\begin{pmatrix}\hat{u}^0\\ \hat{v}^0\end{pmatrix}\right)+\hat{f}\left(-W\hat{u}^1_{\hat{z}}+\hat{v}^1+N\hat{u}^1_{\hat{z}\hat{z}}\right). \tag{5.21}$$

From Section 5.3.1 it was determined that the linear operator in the above equation which concerns wind speeds $\hat{u}^0$ and $\hat{v}^0$ is equal to 0. This turns Equation (5.21) into

$$L^v\left(\begin{pmatrix}\hat{u}^0+\hat{f}\hat{u}^1\\ \hat{v}^0+\hat{f}\hat{v}^1\end{pmatrix}\right)=+\hat{f}\left(-W\hat{u}^1_{\hat{z}}+\hat{v}^1+N\hat{u}^1_{\hat{z}\hat{z}}\right). \tag{5.22}$$

Next, the non-linear operator

$$N^v\left(\begin{pmatrix}\hat{u}^0+\hat{f}\hat{u}^1\\ \hat{v}^0+\hat{f}\hat{u}^1\end{pmatrix}\right)=\frac{\frac{\hat{v}^0+\hat{f}\hat{v}^1}{\hat{u}^0+\hat{f}\hat{u}^1}}{\sqrt{1+\left(\frac{\hat{v}^0+\hat{f}\hat{v}^1}{\hat{u}^0+\hat{f}\hat{u}^1}\right)^2}}. \tag{5.23}$$

Now the operators with superscript u are studied, first the linear operator

$$L^u\left(\begin{pmatrix}\hat{u}^0+\hat{f}\hat{u}^1\\ \hat{v}^0+\hat{f}\hat{v}^1\end{pmatrix}\right)=L^u\left(\begin{pmatrix}\hat{u}^0\\ \hat{v}^0\end{pmatrix}\right)+\hat{f}\left(W\hat{v}^1_{\hat{z}}+\hat{u}^1-N\hat{v}^1_{\hat{z}\hat{z}}\right). \tag{5.24}$$

A similar argument is used as before. The linear operator concerning the first wind speed term in the summation is known. According to Section 5.3.1 it is equal to 1. This turns Equation (5.24) into

$$L^u\left(\begin{pmatrix}\hat{u}^0+\hat{f}\hat{u}^1\\ \hat{v}^0+\hat{f}\hat{v}^1\end{pmatrix}\right)=1+\hat{f}\left(W\hat{v}^1_{\hat{z}}+\hat{u}^1-N\hat{v}^1_{\hat{z}\hat{z}}\right). \tag{5.25}$$

Lastly, the non-linear operator

$$N^u\left(\begin{pmatrix}\hat{u}^0+\hat{f}\hat{u}^1\\ \hat{v}^0+\hat{f}\hat{u}^1\end{pmatrix}\right)=\frac{1}{\sqrt{1+\left(\frac{\hat{v}^0+\hat{f}\hat{v}^1}{\hat{u}^0+\hat{f}\hat{u}^1}\right)^2}}. \tag{5.26}$$

Before continuing, the non-linear operators are discussed. First, only the non-linear operator with superscript v is studied. This is due to non-linear operator with superscript u being a simpler form of the fraction of the aforementioned operator. Both operators were either a sine or cosine of angle β, which has been discussed in Section 5.2 .The sine equals

$$\sin\beta=\frac{\hat{v}}{\hat{u}}\left(1+\left(\frac{\hat{v}}{\hat{u}}\right)^2\right)^{-\frac{1}{2}}, \tag{5.27}$$

which is just rewriting Equation (5.8). The first term is studied,

$$\frac{\hat{v}}{\hat{u}}=\frac{\hat{v}^0+\hat{v}^1\hat{f}}{\hat{u}^0+\hat{u}^1\hat{f}}=\left(\hat{v}^0+\hat{v}^1\hat{f}\right)\frac{1}{\hat{u}^0}\left(1+\frac{\hat{u}^1}{\hat{u}^0}\hat{f}\right)^{-1}. \tag{5.28}$$

Using the binomial theorem, the last term in Equation (5.28) will equal

$$\left(1+\frac{\hat{u}^1}{\hat{u}^0}\hat{f}\right)^{-1}=1-\frac{\hat{u}^1}{\hat{u}^0}\hat{f}+\left(\frac{\hat{u}^1}{\hat{u}^0}\right)^2\hat{f}^2+\mathcal{O}\left(\hat{f}^3\right). \tag{5.29}$$

So in total:

$$\frac{\hat{v}}{\hat{u}}=\frac{1}{\hat{u}^0}\left(\hat{v}^0+\hat{f}\left(\hat{v}^1-\frac{\hat{u}^1\hat{v}^0}{\hat{u}^0}\right)+\mathcal{O}(\hat{f}^2)\right) \tag{5.30}$$

In the above equation, all terms of order $\mathcal{O}(\hat{f}^2)$ will drop out, as only the first order problem is studied.

$$\hat{f}\frac{\hat{v}}{\hat{u}} = \hat{f}\left(\hat{v}^0 + \hat{v}^1\hat{f}\right)\frac{1}{\hat{u}^0}\left(1 - \frac{\hat{u}^1}{\hat{u}^0}\hat{f} + \left(\frac{\hat{u}^1}{\hat{u}^0}\right)^2\hat{f}^2 + \mathcal{O}\left(\hat{f}^3\right)\right) = \hat{f}\frac{\hat{v}^0}{\hat{u}^0}. \tag{5.31}$$

A closer look at the square root yields

$$\hat{f}\left(1 + \left(\frac{\hat{v}}{\hat{u}}\right)^2\right)^{-\frac{1}{2}} = \hat{f}^2\left(\sqrt{\hat{f}^2\left(1 + \left(\frac{\hat{v}}{\hat{u}}\right)^2\right)}\right)^{-1} = \hat{f}^2\left(\sqrt{\hat{f}^2 + \left(\hat{f}\frac{\hat{v}}{\hat{u}}\right)^2}\right)^{-1}, \tag{5.32}$$

$$= \hat{f}^2\left(\sqrt{\hat{f}^2 + \left(\hat{f}\frac{\hat{v}^0}{\hat{u}^0}\right)^2}\right)^{-1} = \hat{f}^2\left(\hat{f}\sqrt{1 + \left(\frac{\hat{v}^0}{\hat{u}^0}\right)^2}\right)^{-1}, \tag{5.33}$$

$$= \hat{f}\left(1 + \left(\frac{\hat{v}^0}{\hat{u}^0}\right)^2\right)^{-\frac{1}{2}}. \tag{5.34}$$

Hence,

$$\hat{f}\sin\beta = \hat{f}\frac{\frac{\hat{v}^0}{\hat{u}^0}}{\sqrt{1 + \left(\frac{\hat{v}^0}{\hat{u}^0}\right)^2}}, \tag{5.35}$$

and therefore,

$$\hat{f}\cos\beta = \hat{f}\frac{1}{\sqrt{1 + \left(\frac{\hat{v}^0}{\hat{u}^0}\right)^2}}. \tag{5.36}$$

Thus, the non-linear operator with superscript v multiplied with $\hat{f}$ will equal the following

$$\hat{f}N^{\hat{v}}\left(\begin{pmatrix}\hat{u}^0 + \hat{f}\hat{u}^1\\ \hat{v}^0 + \hat{f}\hat{u}^1\end{pmatrix}\right) = \hat{f}\frac{\frac{\hat{v}^0}{\hat{u}^0}}{\sqrt{1 + \left(\frac{\hat{v}^0}{\hat{u}^0}\right)^2}}, \tag{5.37}$$

and the other non-linear operator multiplied with $\hat{f}$ will equal

$$\hat{f}N^{u}\left(\begin{pmatrix}\hat{u}^0 + \hat{f}\hat{u}^1\\ \hat{v}^0 + \hat{f}\hat{u}^1\end{pmatrix}\right) = \hat{f}\frac{1}{\sqrt{1 + \left(\frac{\hat{v}^0}{\hat{u}^0}\right)^2}}. \tag{5.38}$$

Equation (5.22), Equation (5.26), Equation (5.37) and Equation (5.38) are put together, which gives

$$\begin{aligned}\hat{f}\left(-W\hat{u}_{\hat{z}}^1 + \hat{v}^1 + N\hat{u}_{\hat{z}\hat{z}}^1\right) &= \hat{f}\frac{\frac{\hat{v}^0}{\hat{u}^0}}{\sqrt{1 + \left(\frac{\hat{v}^0}{\hat{u}^0}\right)^2}},\\ 1 + \hat{f}\left(W\hat{v}_{\hat{z}}^1 + \hat{u}^1 - N\hat{v}_{\hat{z}\hat{z}}^1\right) &= 1 + \hat{f}\frac{1}{\sqrt{1 + \left(\frac{\hat{v}^0}{\hat{u}^0}\right)^2}}.\end{aligned} \tag{5.39}$$

The above system can be simplified to

$$\begin{aligned}W\hat{u}_{\hat{z}}^1 + \hat{v}^1 + N\hat{u}_{\hat{z}\hat{z}}^1 &= -\frac{\frac{v^0}{\hat{u}^0}}{\sqrt{1 + \left(\frac{\hat{v}^0}{\hat{u}^0}\right)^2}},\\ W\hat{v}_{\hat{z}}^1 + \hat{\hat{u}}^1 - N\hat{v}_{\hat{z}\hat{z}}^1 &= \frac{1}{\sqrt{1 + \left(\frac{\hat{v}^0}{\hat{u}^0}\right)^2}}.\end{aligned} \tag{5.40}$$

Generally, the above system can be rewritten to

$$\dot{\mathbf{u}}(\hat{z}) = A\mathbf{u}(\hat{z}) + \mathbf{F}(\hat{z}), \tag{5.41}$$

where the dot represents a derivative with respect to the non-dimensional height and

$$\mathbf{u} = \begin{pmatrix} \hat{u}^1 \\ \mu \\ \hat{v}^1 \\ \nu \end{pmatrix}, \tag{5.42}$$

with $\mu = \hat{u}^1_{\hat{z}}$ and $\nu = \hat{v}^1_{\hat{z}}$. Then, A is a matrix which contains the linear part of the system given in Equation (5.40). Matrix A will equal

$$A = \frac{1}{N}\begin{pmatrix} 0 & N & 0 & 0 \\ 0 & -W & -1 & 0 \\ 0 & 0 & 0 & N \\ 1 & 0 & 0 & W \end{pmatrix}. \tag{5.43}$$

Lastly, $\mathbf{F}(\hat{z})$ indicated the non-linear terms on the system of equations. The function depends only on the non-dimensional height, as $\hat{u}^0$ and $\hat{v}^0$ are known solutions which depend on $\hat{z}$. The function is defined as

$$\mathbf{F}(\hat{z}) = \frac{1}{N}\begin{pmatrix} 0 \\ \frac{\hat{v}^0}{\hat{u}^0} \\ \sqrt{1+\left(\frac{\hat{v}^0}{\hat{u}^0}\right)^2} \\ 0 \\ \frac{1}{\sqrt{1+\left(\frac{\hat{v}^0}{\hat{u}^0}\right)^2}} \end{pmatrix}. \tag{5.44}$$

Solving the matrix vector differential equation given in Equation (5.41) is done via the method of variation of parameters.

Generally speaking, the method of variation of parameters helps to find the solution of a nonhomogeneous equation by studying the homogeneous version. In the homogeneous version of the problem, the constants are determined which appear during the usage of the superposition principle. In the case of Equation (5.41), the solution of the homogeneous version can be written as

$$\mathbf{u}_{\text{hom}}(\hat{z}) = \Phi(\hat{z})\mathbf{c}, \tag{5.45}$$

where Φ represents the fundamental matrix and $\mathbf{c}$ is a vector containing the constants belonging to the solutions of the homogeneous problem. The next step is crucial to the method of variation of parameters, it is assumed that the constants depend on the independent variable. In this case, this would mean that $\mathbf{c}$ will depend on the non-dimensional height, so

$$\mathbf{u} = \Phi(\hat{z})\mathbf{c}(\hat{z}). \tag{5.46}$$

Substituting the above solution into the original nonhomogeneous Equation (5.41), gives

$$\dot{\mathbf{u}} = \dot{\Phi}(\hat{z})\mathbf{c}(\hat{z}) + \Phi(\hat{z})\dot{\mathbf{c}}(\hat{z}) = A\Phi(\hat{z})\mathbf{c}(\hat{z}) + \mathbf{F}(\hat{z}), \tag{5.47}$$

and since the fundamental matrix has the property that $\dot{\Phi}(\hat{z}) = A\Phi(\hat{z})$, it will hold that

$$\Phi(\hat{z})\dot{\mathbf{c}}(\hat{z}) = \mathbf{F}(\hat{z}). \tag{5.48}$$

As the fundamental matrix consists of columns which contain linearly independent solutions at every height, its inverse exists. Therefore,

$$\dot{\mathbf{c}}(\hat{z}) = \Phi^{-1}(\hat{z})\mathbf{F}(\hat{z}). \tag{5.49}$$

The above expression is integrated between a certain height $\hat{z}_0$ and $\hat{z}$ to obtain

$$\mathbf{c}(\hat{z}) = \mathbf{c}(\hat{z}_0) + \int_{\hat{z}_0}^{\hat{z}} \Phi^{-1}(s)\mathbf{F}(s)\mathrm{d}s. \tag{5.50}$$

Note that $\mathbf{c}(\hat{z}_0)$ can be rewritten using the fundamental matrix to get

$$\mathbf{c}(\hat{z}) = \Phi^{-1}(\hat{z}_0)\mathbf{u}(\hat{z}_0) + \int_{\hat{z}_0}^{\hat{z}} \Phi^{-1}(s)\mathbf{F}(s)\mathrm{d}s. \tag{5.51}$$

As the interest is in the wind speed, and not in the constants, using Equation (5.46), the following is obtained

$$\mathbf{u} = \Phi(\hat{z})\Phi^{-1}(\hat{z}_0)\mathbf{u}(\hat{z}_0) + \Phi(\hat{z}) \int_{\hat{z}_0}^{\hat{z}} \Phi^{-1}(s)\mathbf{F}(s)\mathrm{d}s. \tag{5.52}$$

It should be noted that the integral in Equation (5.52) will likely be impossible to integrate, due to the exponential, sines and cosines in the non-linear function $\mathbf{F}$. Hence, a numerical approximation, like the mid-point rule, of the integral should then be used to gain an expression of the analytical solution for the wind speed.

Above expression could be worked out further, as the fundamental matrix is equal to the matrix exponential of the matrix given in Equation (5.43). However, this expression is too big to write down to fit on this page.

The above described algorithm can be applied to obtain the analytical solution of the Ekman spiral containing vertical wind speed with a general perturbation method up to order $\mathcal{O}(\hat{f})$.

5.4. Numerical scheme for Ekman Spiral with Vertical Wind Speed

When not using the algorithm for the analytical solution given in Section 5.3, a numerical scheme is used to solve Equation (5.5). The numerical method chosen for the hodograph is elaborated in this section.

The numerical scheme chosen in this report is Euler Forward, an explicit method. To use this method, the equations of motion are first rewritten using the following

$$\mathbf{w} = \begin{pmatrix} \hat{u} \\ \hat{u}_{\hat{z}} \\ \hat{v} \\ \hat{v}_{\hat{z}} \end{pmatrix}. \tag{5.53}$$

In the Forward Euler method, the values for the equations of motion are computed using a straightforward vector-valued method given in Equation (5.54)

$$\mathbf{w}_{n+1} = \mathbf{w} + \Delta t \mathbf{f}(\hat{z}_n, \mathbf{w}_n). \tag{5.54}$$

In the above equation, $\mathbf{f}$ is defined as the following function

$$\mathbf{f}(\hat{z}_n, \mathbf{w}_n) = \begin{pmatrix} \hat{u}_{\hat{z}} \\ \frac{1}{N}\left(W\hat{u}_{\hat{z}} - \hat{v} + F\frac{\frac{\hat{v}}{\hat{u}}}{\sqrt{1+\left(\frac{\hat{v}}{\hat{u}}\right)^2}} \right) \\ \hat{v}_{\hat{z}} \\ \frac{1}{N}\left(W\hat{v}_{\hat{z}} - 1 + \hat{u} - F\frac{1}{\sqrt{1+\left(\frac{\hat{v}}{\hat{u}}\right)^2}} \right) \end{pmatrix}. \tag{5.55}$$

Thus the numerical method used to visualize the non-dimensional wind speeds $\hat{u}$ and $\hat{v}$ has now been determined. The Forward Euler method is chosen due to its simplicity. More difficult numerical methods could be used, suggestions are given in Section 6.3. The shortcoming of the Forward Euler method, is it high order of truncation error when comparing it to other numerical methods.

Also, there is a difficulty in implementing the above numerical method. In the definition of $\mathbf{f}(\hat{z}_n, \mathbf{w}_n)$, a fraction appears which divided $\hat{v}$ and $\hat{u}$. As the starting point of the hodograph is $(0, 0)$, the wind speed at ground level, function $\mathbf{f}(\hat{z}_n, \mathbf{w}_n)$ will not be defined here. It is therefore assumed that around the starting point of the hodograph, both wind speeds behave according to the modified linear Ekman spiral.

This area around the starting point is to be determined in the Section 5.5, which visualized the hodograph using the method discussed in this section.

5.5. Visualization of the Ekman Spiral with Vertical Wind Speed

This section visualizes the Ekman spiral with vertical wind speed. The visualization of the hodograph is made with the numerical scheme discussed in Section 5.4. After that, the influence of the different parameters will be discussed.

Due to the numerical scheme, the first step before discussing the influence of the different parameters on the equations of motion, is to visualize the general form of the hodograph first. This means the base hodograph to which the hodograph with varying parameters will be compared.

As discussed previously, due to the non-linearity the hodograph of the Ekman spiral with vertical wind speed cannot start in the starting point $(0, 0)$. Hence, at first the modified linear Ekman spiral is used. The point where the Ekman vertical wind speed takes over from the modified linear Ekman spiral is defined as the turning point. The following figure visualizes hodographs with different turning points. This is done to select the best turning point for the hodographs.

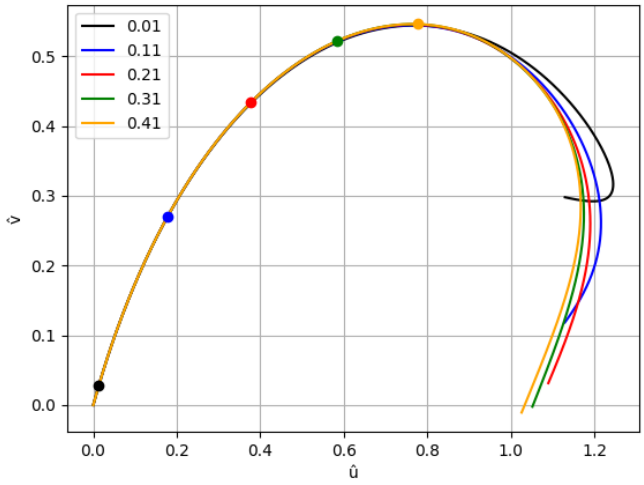

Figure 5.1: Hodographs of the Ekman spiral with vertical wind speed each having a different starting point from 0.01 up to 0.51 where the linear solution ends and the numerical schema starts.

In Figure 5.1 the hodograph with different turning points is visualized. The different colored lines correspond to the value of the turning point. The exact point where the Ekman spiral with vertical wind speed takes over from the modified linear Ekman spiral is indicated by the same colored dot.

For higher turning points, the hodograph comes closer to the required end point $(1, 0)$. However, this means that there is more influence of the modified linear Ekman spiral on the Ekman spiral with vertical wind speed. This will thus give a distorted image of how the Ekman spiral with vertical wind speed will act. Therefore, a low turning point is desirable.

To decide which turning point is used for the visualization, the start of the hodograph is studied. Up until the first black dot, the hodograph appears to move in a linear line. The angle under which the hodographs moves away from the starting point, is determined by the modified linear Ekman spiral. It can be assumed that the Ekman spiral will only differ slightly from this angle, which is why the turning point will be chosen as 0.01.

Note that the Ekman spiral with vertical wind speed does not end up in the point where it should. It should end exactly in the point $(1, 0)$. Therefore, there is a *shooting problem*. By giving minor perturbations in the direction of both wind speeds, the hodograph should end up in the desired end point.

Firstly, in Figure 5.1 it can be seen that the wind speed v is farthest away from the desired point, being at 0.3 whereas it should be at 0. Therefore, the perturbation in wind speed v will be studied first.

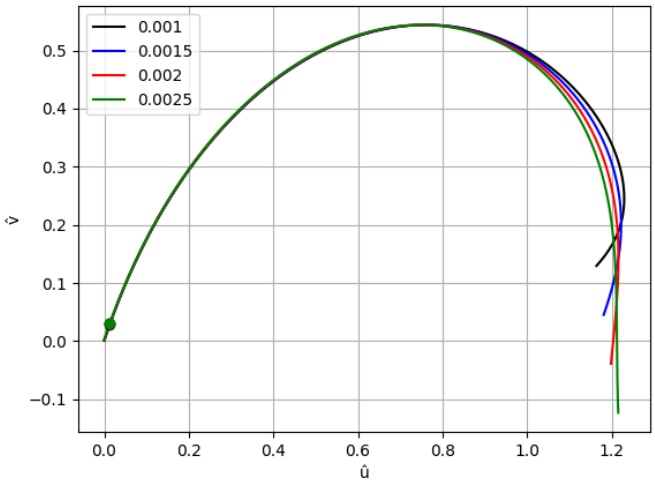

Figure 5.2: Hodographs with different perturbations in wind speed v, perturbation in u equal to 0 and turning point 0.1.

In Figure 5.2 it can be seen that the red and green hodographs do not go towards the desired end point. The same is true for the black line. Hence, the perturbation in wind speed v which coincides with the blue hodograph is chosen to solve the shooting problem.

Next, as wind speed u is also still not at the end point, a minor perturbation parameter is also introduced the this wind speed. This is again visualized in several hodographs, with wind speed v chosen equal to 0.0015.

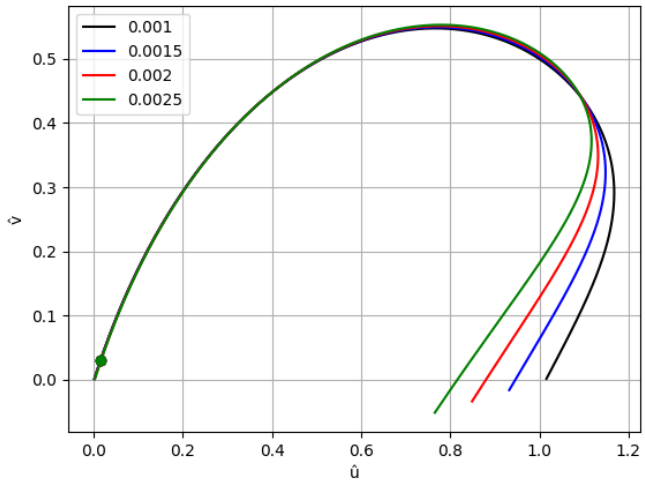

Figure 5.3: Hodographs with different perturbation in u with the perturbation in v equal to 0.0015 and turning point 0.1.

In Figure 5.3 it can be seen that the black hodograph with perturbation 0.001 ends up in the correct end point. The other hodographs all end up beyond the desired end point.

Some minor alterations are done to the perturbation parameters; the perturbation in v is put equal to 0.00155 and u is equal to 0.0011. For these perturbation values, the hodograph gets even closer to the end point. The hodograph with these parameter values can be seen in the Figure 5.4.

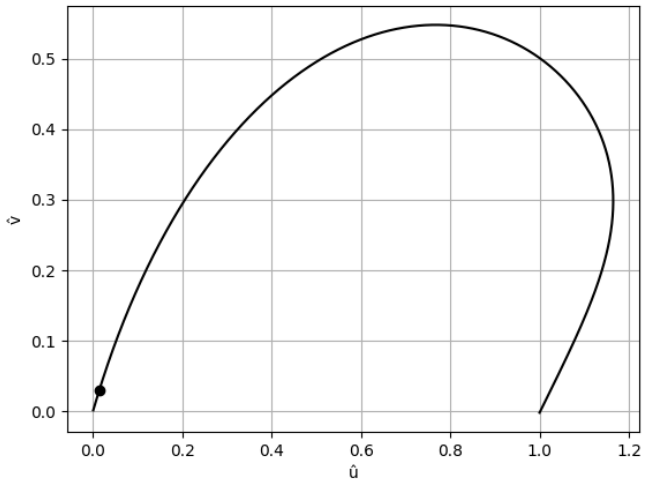

Figure 5.4: Hodograph of the Ekman spiral with vertical wind speed with turning point 0.1, a perturbation in u equal to 0.0011 and perturbation is v chosen equal to 0.00155.

Now that the different perturbations values and the turning point for the hodograph have been chosen, a further analysis can be done on the influence of the different parameters on the hodograph for the Ekman spiral with vertical wind speed. Only a new parameter F, which consists of $\hat{f}$, f and $\hat{w}$, is introduced as compared to the modified linear Ekman spiral. Therefore, the influence of these three parameters is crucial to the behaviour of the Ekman spiral with vertical wind speed.

However, due to the simple approximation, the numerical scheme and turning point, to the non-linear problem, the shooting problem which occurs makes it unable to analyze the influence of all the parameters. Each parameter will namely make the hodograph change in end point. As the perturbation parameters are chosen to make the hodograph end in the required end point, these perturbation parameters will influence the other parameters. Therefore, the effect of the other parameters on the hodograph cannot be studied.

The Python code used to create Figure 5.1, Figure 5.2, Figure 5.3 and Figure 5.4 can be found in Appendix E.

5.5.1. Comparing Modified Linear Ekman Spiral and Ekman Spiral with Vertical Wind Speed

The modified linear Ekman spiral and the Ekman spiral with vertical wind speed are compared in this section. These two Ekman spirals are compared in the same way as in Section 4.4.1.

The different errors in wind speed u and v are similar to ε_u and ε_v, only now the modified linear Ekman spiral and the Ekman spiral with vertical wind speed. Thus, now the error in wind speed u is defined as

$$\hat{\varepsilon_u} = \sum_{\hat{i}=1}^{10^5} |\hat{u}(\hat{i}) - \hat{u}_c(\hat{i})|. \tag{5.56}$$

In the above equation, the parameter $\hat{i}$ is defined

$$\hat{i} = \frac{i}{10^5}, \tag{5.57}$$

so that values of both non-dimensionalized wind speeds u of Ekman's spiral are calculated at a certain height. By subtracting these from each other, the error becomes smaller when the two hodographs have more overlap. The error in wind speed v is defined as

$$\hat{\varepsilon_v} = \sum_{\hat{i}=1}^{10^5} |\hat{v}(\hat{i}) - \hat{v}_c(\hat{i})|. \tag{5.58}$$

In the following figure, the hodographs of the two different spirals can be seen. The black dot still represents the turning point of the Ekman spiral with a constant vertical wind speed.

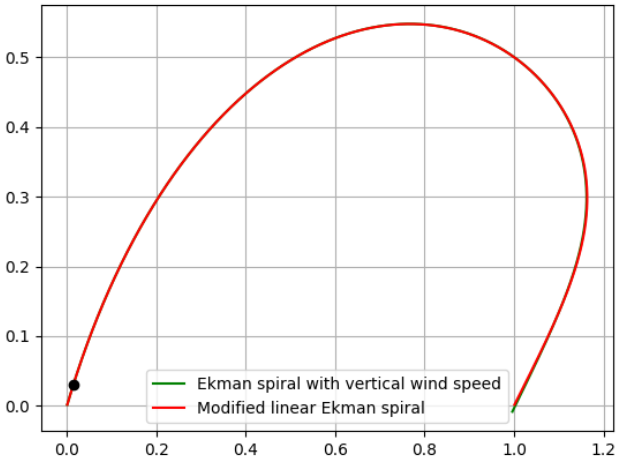

Figure 5.5: Hodographs of the modified linear Ekman spiral and the Ekman spiral with constant vertical wind speed, with parameter values as discussed previously.

It can be seen that the hodographs overlap almost everywhere. Only near the end the difference between the two hodographs can be seen. For above hodograph, the value of the previously defined error in wind speed u indicated by parameter $\hat{\varepsilon}_u$ is equal to

$$\hat{\varepsilon}_u = 14337, \tag{5.59}$$

the error in the other wind speed equals

$$\hat{\varepsilon}_v = 11522. \tag{5.60}$$

For higher values of the ABL, the error increases rapidly for both wind speed u and v. This can be seen in the following figure.

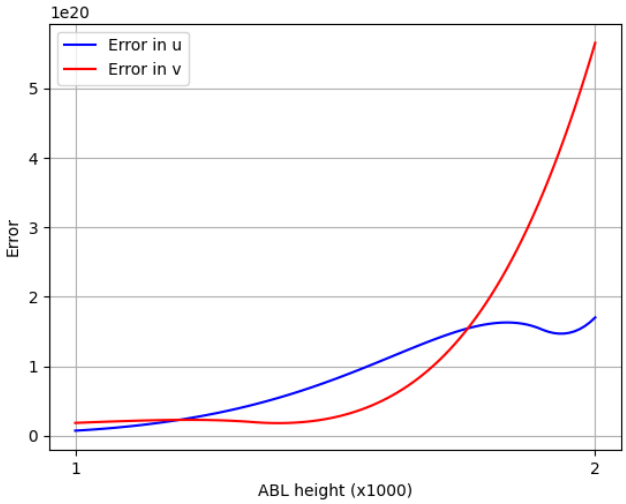

Figure 5.6: The error of the wind speed u and v between the modified linear Ekman spiral and the Ekman spiral with a vertical wind speed.

In Figure 5.6 the error is very large at the ABL height of a thousand metres, but increases more by increasing the ABL height. The error in wind speed v especially seemingly grows exponentially, whereas

the wind speed u does not grow as fast. For even higher values of the ABL, the error increases even more upwards to order 10^{27}.

The increase in error, as opposed to the decrease in error when comparing the classical Ekman spiral and the modified linear Ekman spiral, can be attributed to the shooting problem which occurs when visualizing the Ekman spiral with a constant vertical wind speed. This shooting problem is solved for an ABL height with certain perturbation parameters. Thus, when the ABL height increases but the perturbation parameters do not change, the error will increase. The code for creating Figure 5.6 can be seen in Appendix B.2.

5.6. Conclusion on Analysis of Ekman Spiral with Vertical Wind Speed

This section will conclude on the Ekman spiral with constant vertical wind speed. A short overview of the assumptions, boundary conditions, analytic algorithm and numerical scheme are discussed. For reasons mentioned in Section 5.5, the influence of the different parameters is not discussed as this was not studied.

Compared to the previously discussed version of the Ekman spiral, the only changed assumption is the one discussing the vertical Coriolis parameter. It was assumed that this parameter was equal to zero, when discussing the modified linear Ekman spiral. However, the Ekman spiral with vertical wind speed no longer has this assumption.

There is no change in the boundary conditions compared to the modified linear Ekman spiral. Therefore, there are no other remarks about the boundary conditions when discussing the Ekman spiral with vertical wind speed.

The hodograph of the Ekman spiral with a constant vertical wind speed can be visualized using either the algorithm discussed previously in Section 5.3 or the numerical scheme discussed in Section 5.54. The analytic algorithm consists of using a RPM for solving the equations of motion, in which a difficulty lies in the non-linear part. The algorithm has been worked out up to order $\mathcal{O}\left(\hat{f}\right)$.

The numerical scheme used to visualize the hodograph of the Ekman spiral with a vertical wind speed is the Euler explicit method. Due to the non-linearity of the equations of motion for this Ekman spiral, there is a shooting problem. The hodograph is shot away from the starting point $(0, 0)$ and different perturbation parameters are chosen so that the hodograph ends up in the desired end point $(1, 0)$. Also, a turning point is introduced, as there will otherwise be a division by 0.

In conclusion, the Ekman spiral with a constant vertical wind speed is in theory an even more realistic model for studying the wind flow when comparing it to the modified linear Ekman spiral. Due to the non-linearity in the equations of motion, this problem is much harder to solve than the other spirals discussed in this thesis. All the different parameters in the equations of motion can be reduced to three parameters in total, two of which already appeared in the modified linear Ekman spiral. The shortcoming of this spiral lies in the numerical scheme used. Due to the shooting problem, the influence of the parameters can not be discussed.

6

Conclusions and Recommendations

In this chapter, a short summary of the thesis is given. In Section 6.1 this summary is given. Next, as there is still work to be done on improving the Ekman spiral, several recommendations for future work are given in the sections that follow the first section; in Section 6.2 the possibility for an analytical solution of the Ekman spiral with vertical wind speed is discussed, in Section 6.3 other numerical methods to visualize the Ekman spiral with vertical wind speed are recommended. In Section 6.4 the boundary conditions imposed on the Ekman spiral are discussed, together with the possibility to change them and lastly, in Section 6.5 the assumptions that were made in this report are discussed. Also, the possibility to change these assumptions or even disregard some of these assumptions are reviewed.

6.1. Summary

This report aimed to extend on a previous thesis (de Jong, 2021) and study the Ekman spiral with a constant vertical wind speed. The previous thesis discussed a modified version of the Ekman spiral which also allowed constant vertical wind speed, but no vertical Coriolis component.

The previous thesis has been extended so that now the modified linear Ekman spiral does coincide exactly with the boundary conditions. The hodograph produced by the wind speeds of this Ekman spiral varies heavily per chosen parameters. Also, there are numerical shortcomings to visualizing the hodograph due to exponents in the solution for wind speeds. These shortcomings occur when the vertical wind speed increases or the ABL height decreases beyond a certain threshold value.

Next, the Ekman spiral with a constant vertical wind speed was studied. Due to the non-linearity, a numerical scheme was used to visualize the hodograph. An algorithm for the analytical approach is given, but not implemented due to the time limit on this thesis. This algorithm is based on a RPM and worked out towards order $\mathcal{O}\left(\hat{f}\right)$. To solve for this order, a varation of parameters method is used, where likely a numerical integration method should be used to work out the integral which appears.

The numerical scheme used for this version of the Ekman spiral, gave rise to a shooting problem when visualizing the Ekman spiral. With a chosen turning point, and different perturbations in the solution for the wind speeds, the shooting problem has been resolved and a visualization has been produced.

6.2. Analytical solution Ekman spiral with Vertical Wind Speed

The analytical solution of the Ekman spiral with a constant vertical wind speed is a crucial aspect which should be studied in further research. The algorithm that has been discussed in Section 5.3, should definitely be implemented to visualize the hodograph of this Ekman spiral.

Further research should decide on which numerical integration method will be used to solve the integrals in the RPM. The numerical integration method should be used, so that the error made is as low as possible. One should also study the possibility of solving this integral analytically, but it is expected that this will not be possible.

Also, the influence of the different parameters should be studied once a hodograph of the Ekman spiral with a constant vertical wind speed has been visualized. Especially the parameter $\hat{f}$ is of interest. When the vertical Coriolis parameter increases, so will the influence of the non-linear term on the

equations of motion. When the vertical Coriolis parameter decreases, the Ekman spiral with vertical wind speed will behave as the modified linear Ekman spiral.

6.3. Numerical methods for Hodograph Ekman Spiral with Vertical Wind Speed

A different numerical method could be used to visualize the hodograph for the Ekman spiral with vertical wind speed. Explicit methods are highly recommended, due to the non-linear term in the equations of motion. Using a different numerical method increases the order of the local truncation error. Several methods, with their truncation error are proposed in Table 6.1 below.

Table 6.1: Several explicit numerical methods with their amplification factor, stability conditions and truncation error.

Method	Amplification factor	Stability condition	Truncation error
Explicit Euler	$1+\lambda\Delta t$	$\Delta t \leq -\frac{2}{\lambda}$	$\mathcal{O}(\Delta t)$
Modified Euler	$1+\lambda\Delta t+\frac{1}{2}(\lambda\Delta t)^2$	$\Delta t \leq -\frac{2}{\lambda}$	$\mathcal{O}\left((\Delta t)^2\right)$
Runge-Kutta-4	$1+\lambda\Delta t+\frac{1}{2}(\lambda\Delta t)^2+\frac{1}{6}(\lambda\Delta t)^3+\frac{1}{24}(\lambda\Delta t)^4$	$\Delta t \leq -\frac{2.8}{\lambda}$	$\mathcal{O}\left((\Delta t)^4\right)$

In Table 6.1, it can clearly be seen that Explicit Euler's method has a higher truncation error when compared to the other explicit methods. Hence, it is recommended that further research takes this into account by implementing the Runge-Kutta-4 method for the visualization. This would decrease the truncation error and thus give a more accurate visualization of the hodograph of the Ekman spiral with vertical wind speed.

To solve the shooting problem which occurred when visualizing the Ekman spiral with a constant vertical wind speed, another method then used in this report could be used. There are two different methods which will be discussed.

Now, the hodograph is shot away from the starting point $(0,0)$ with also adding different perturbations in both horizontal wind speeds. These perturbations were chosen to make the hodograph end up in the correct end point $(1,0)$. Also, currently a turning point is used, as otherwise a division by 0 happens in the non-linear part of the equations of motion.

Another method to solve the shooting problem, is to make the hodograph shoot away from the end point. In this point, there will be no problem with the non-linear term in the equations of motion of the Ekman spiral with a constant vertical wind speed, so no turning point at the start is required. At the starting point, there still is a problem with a division by 0. Therefore, still a turning point is required at the end of the hodograph, as well as some minor perturbations in both horizontal wind speeds.

One could also make the hodograph shoot away from both the starting point and the end point. From the starting point, a turning point is still required. However, now perturbations can be modified in four parameters. Two for each hodograph which is shot away from a point.

Further research could delve into one or multiple of these options of different methods for solving the shooting problem which occurs when numerically visualizing the Ekman spiral with a constant vertical wind speed.

6.4. Boundary conditions of the Ekman spiral

The boundary conditions which are currently imposed on the Ekman spiral involve the height of the ABL. The height of the ABL has a major influence on the behaviour of the hodograph, but the specific height for the ABL is not known. Therefore, the boundary conditions could be changed so that the ABL has less of a major role.

The suggested way to implement the boundary conditions in further research is to define a beam in $\mathbb{R}^3$. The boundary conditions should be imposed on the boundary of this beam. Currently, only boundary conditions are imposed on wind speed u and v. However, when defining a beam, boundary conditions can also be imposed on the vertical wind speed w. The exact behaviour of the wind can be studied within the beam when using this construction.

Also, using the beam method, one could try to use a separation of variables method if one takes the vertical wind speed to be small. Using the separation of variables method, the process of solving

the equations of motion for the wind speed should be a more straight forward process.

6.5. Discussion on Assumptions

There were several assumptions made on the equations of motion originally given in Chapter 2 and on the vertical wind speed in Chapter 5. Also, several assumptions were made on the parameter values in Section 2.6. Some of these assumptions can be changed of even disregarded without drastically altering the solution method. However, there are assumptions which do significantly change the way to obtain a solution of the equations of motion if they are reversed.

Assumptions which can be reversed with little to no change to the solution method are discussed first. The first easily reversible assumption is about the gravitational constant. This constant can be allowed to vary with the latitude of the earth. This will not change the solution if the vertical wind speed remains constant. Having a constant vertical wind speed makes sure that the equation concerning the vertical wind speed in the equations of motion is still of no importance to the solution of the horizontal wind speeds, as each vertical wind speed term where a derivative is taken with respect to the height drops out.

Another assumption that could be reversed is the assumption that the geostrophic wind speed does not depend on height. If the geostrophic wind is assumed to be a linear function dependent on the height, generally $\bar{u}(\hat{z}) = a_0 + a_1\hat{z}$, the non-dimensionalization is adjusted by the constant a_1. The boundary conditions remain the same.

Assumptions which are harder to reverse are those concerning the wind speeds in the equation of motion. There are two major assumptions which are shortly discussed.

The assumption that there is a steady flow could be partially disregarded. A steady flow which is for example periodic, could be implemented as well. This will add a term on all equations of motion which varies in a known way in time. If the wind speed does not vary in a known way with time, another independent variable is introduced into the equations of motion. This will make the equations even harder to solve.

Allowing a non constant vertical wind speed makes the equations of motion have three equations. This will make the hodograph for the different wind speeds three-dimensional. The equation concerning the vertical wind speed is not likely to pose problems for solving for the vertical wind speed. However, due to the non-linearity that exists in the other equations in the system, a numerical schema might still be preferable.

Bibliography

Anderson-Jr, J. D. (1978). *Introduction to Flight*. McGraww-Hill.

AWEA (2010). Wind energy basics. https://web.archive.org/web/20100923194211-http://www.awea.org/faq/wwt_basics.html (Accessed: 01-07-2021).

de Jong, A. L. (2021). Application of matching to arrive a wind shear relation for the entire atmospheric boundary layer. *Master's thesis. Delft University of Technology, the Netherlands*.

Doering, C. and Gibbon, J. (1995). *Applied Analysis of the Navier-Stokes Equations*. Cambridge University Press.

Ekman, W. (1905). On the influence of the earth's rotation on ocean-currents. *Arkiv For Matematik, Astronomi och Fysik*, 2.

Elert, G. (2009). Angular speed of the earth. https://hypertextbook.com/facts/2002/JasonAtkins.shtml (Accessed: 01-07-2021).

Emeis, S. (2018). *Wind Energy Meteorology: Atmospheric Physics for Wind Power Generation*. Springer.

ESA (2021). Gravity in detail. https://earth.esa.int/web/guest/missions/esa-operational-eo-missions/goce/content/-/asset_publisher/TA2e/content/gravity-in-detail-5728 (Accessed: 01-07-2021).

Hakim, G. and Holton, J. (2012). *An Introduction to Dynamic Meteorology*. Academic Press.

MapsOfWorld (2017). Maps of world. https://www.mapsofworld.com/lat_long/netherlands-lat-long.html (Accessed: 01-07-2021).

Parker, D. (2003). *Fileds, Flows and Waves; an Introduction to Continuum Models*. Springer.

Roussey, B. (2021). Bigger wind turbines are on the horizon. https://www.cleanenergyauthority.com/solar-energy-news/bigger-wind-turbines-are-horizon-043021 (Accessed: 01-07-2021).

Zhang, J., Chen, H., Zhu, Y., Shi, H., Zheng, Y., Xia, X., Teng, Y., Wang, F., Han, X., Li, J., and Xuan, Y. (2019). A novel method for estimating the vertical velocity of air with a descending radiosonde system. *Remote Sensing*, 11(13).

Appendices

A

Determining Constants Modified Linear Ekman Spiral

A.1. Matrix Representation Modified Linear Ekman Spiral

The following system is studied

$$A\mathbf{b} = \mathbf{x}, \tag{A.1}$$

where

$$A = \begin{pmatrix} \mathrm{e}^{p}\cos(q) - \mathrm{e}^{k}\cos(q) & \mathrm{e}^{p}\sin(q) & \mathrm{e}^{k}\sin(q) \\ W(p-k) - N\left(p^2 - k^2\right) & Wq - 2Npq & Wq - 2Nkq \\ a_{3,1} & a_{2,3} & a_{3,3} \end{pmatrix}, \tag{A.2}$$

with

$$\begin{aligned} a_{3,1} = {} & W\left(\mathrm{e}^{p}\left(p\cos(q) - q\sin(q)\right) + \mathrm{e}^{k}\left(q\sin(q) - k\cos(q)\right)\right) \\ & - N\left(\mathrm{e}^{p}\left(\cos(q)\left(p^2 - q^2\right) - 2pq\sin(q)\right) - \mathrm{e}^{k}\left(\cos(q)\left(k^2 - q^2\right) - 2kq\sin(q)\right)\right), \end{aligned} \tag{A.3}$$

also

$$a_{2,3} = W\mathrm{e}^{p}\left(p\sin(q) + q\cos(q)\right) - N\mathrm{e}^{p}\left(\sin(q)\left(p^2 - q^2\right) + 2pq\cos(q)\right), \tag{A.4}$$

and

$$a_{3,3} = W\mathrm{e}^{k}\left(k\sin(q) + q\cos(q)\right) - N\mathrm{e}^{k}\left(\sin(q)\left(k^2 - q^2\right) + 2kq\cos(q)\right). \tag{A.5}$$

The vector **b** consists of the three remaining constants, see Equation (A.6)

$$\mathbf{b} = \begin{pmatrix} b_1 \\ b_2 \\ b_4 \end{pmatrix}. \tag{A.6}$$

Remaining vector **x** consists of the three values on the boundary

$$\mathbf{x} = \begin{pmatrix} 0 \\ 1 \\ 0 \end{pmatrix}. \tag{A.7}$$

A.2. Python Code implementation determining constants

```
import numpy as np

def constantebepaling(N,W):
    a = (W**2)/(4*(N**2))
    b = 1/N
    r = np.sqrt(np.sqrt((a**2)+(b**2)))
    phi = np.sqrt((1+(W**2)/(4*(N**2)*(r**2)))/2)
    theta = np.sqrt((1-(W**2)/(4*(N**2)*(r**2)))/2)
    p = W/(2*N)+r*phi
    q = r*theta
    k = W/(2*N)-r*phi

    A = np.array([[np.exp(p)*np.cos(q)-np.exp(k)*np.cos(q), np.exp(p)*np.
        ↪ sin(q), np.exp(k)*np.sin(q)],[W*(p-k)-N*((p**2)-(k**2)), W*q-2*N
        ↪ *p*q, W*q-2*N*k*q],[W*(np.exp(p)*(p*np.cos(q)-q*np.sin(q)) - np.
        ↪ exp(k)*(k*np.cos(q)-q*np.sin(q))) - N*(np.exp(p)*(np.cos(q)*((p
        ↪ **2)-(q**2))-2*p*q*np.sin(q))-np.exp(k)*(np.cos(q)*((k**2)-(q
        ↪ **2))-2*k*q*np.sin(q))), W*np.exp(p)*(p*np.sin(q)+q*np.cos(q)) -
        ↪  N*np.exp(p)*(np.sin(q)*((p**2)-(q**2))+2*p*q*np.cos(q)), W*np.
        ↪ exp(k)*(k*np.sin(q)+q*np.cos(q)) - N*np.exp(k)*(np.sin(q)*((k
        ↪ **2)-(q**2))+2*k*q*np.cos(q))]])

    B = np.array([0,1,0])

    Bcon = np.linalg.solve(A, B)

    return Bcon
```

B

Determining error between wind speeds

B.1. Python code for graph of errors in wind speeds classical and modified linear

```
import matplotlib.pyplot as plt
from numpy import sin, cos, exp, sqrt, linspace, array, append
from bepalingconstanten import *

z = linspace(0, 100000, 100000)
zhat = linspace(0, 1, 100000)

stepsize = 50
maxi = 9000 / stepsize

toterru = array([])
toterrv = array([])
err_i = array([])

for i in range(0, int(maxi) + 1):
    err_u = array([])
    err_v = array([])
    ABL = 1000 + stepsize * i
    ubar = 10
    f = 1.1 * 10 ** (-4)
    Km = 5
    N = Km / (f * ABL ** 2)
    what = 0
    W = (what * ubar) / (f * ABL)

    Blist = constantebepaling(N, W)

    b1 = Blist[0]
    b2 = Blist[1]
    b3 = -b1
    b4 = Blist[2]

    a = (W ** 2) / (4 * N ** 2)
    b = 1 / N
    r = sqrt(sqrt(a ** 2 + b ** 2))
    concos = np.sqrt((1 + (W ** 2) / (4 * (N ** 2) * (r ** 2))) / 2)
```

```
    consin = np.sqrt((1 - (W ** 2) / (4 * (N ** 2) * (r ** 2))) / 2)

    p = (W / (2 * N) + r * concos)
    k = (W / (2 * N) - r * concos)
    q = r * consin

    u = ubar - ubar * exp(-(z * sqrt(f)) / sqrt(2 * Km))
        * cos((z * sqrt(f) / sqrt(2 * Km)))
      v = ubar * exp(-(z * sqrt(f)) / sqrt(2 * Km)) * sin((z * sqrt(f)) /
          ↪ sqrt(2 * Km))
    uhat = u / ubar
    vhat = v / ubar

    uw = 1 - W * (p * exp(zhat * p) * (b1 * cos(zhat * q) + b2 * sin(zhat
        ↪ * q)) + exp(p * zhat) * (
            -b1 * q * sin(q * zhat) + b2 * q * cos(q * zhat)) + k * exp(
                ↪ zhat * k) * (
                        b3 * cos(zhat * q) + b4 * sin(zhat * q)) + exp(
                            ↪ zhat * k) * (
                        -b3 * q * sin(q * zhat) + b4 * q * cos(q * zhat)
                            ↪ )) \
          + N * ((p ** 2) * exp(p * zhat) * (b1 * cos(zhat * q) + b2 * sin(
              ↪ zhat * q)) + (k ** 2) * exp(k * zhat) * (
              b3 * cos(zhat * q) + b4 * sin(zhat * q)) + 2 * p * exp(p *
                 ↪ zhat) * (
                        -b1 * q * sin(q * zhat) + b2 * q * cos(q * zhat))
                            ↪ + 2 * k * exp(k * zhat) * (
                        -b3 * q * sin(q * zhat) + b4 * q * cos(q * zhat))
                            ↪ + exp(p * zhat) * (
                        -b1 * (q ** 2) * cos(q * zhat) - b2 * (q ** 2) *
                            ↪ sin(q * zhat)) + exp(k * zhat) * (
                        -b3 * (q ** 2) * cos(q * zhat) - b4 * (q ** 2) *
                            ↪ sin(q * zhat)))

    vw = exp(zhat * p) * (b1 * cos(zhat * q) + b2 * sin(zhat * q)) + exp(
        ↪ zhat * k) * (
            b3 * cos(zhat * q) + b4 * sin(zhat * q))
    vwhat = vw
    uwhat = uw

    for j in range(len(vhat)):
        err_v = append(err_v, abs(vhat[j] - vwhat[j]))

    for j in range(len(uhat)):
        err_u = append(err_u, abs(uhat[j] - uwhat[j]))

    toterru = append(toterru, sum(err_u))
    toterrv = append(toterrv, sum(err_v))
    err_i = append(err_i, i)
    print(ABL)

k_arr = array([])
for k in range(0, len(err_i)):
    if int(1000 + stepsize * err_i[k]) % 1000 == 0:
        k_arr = append(k_arr, k)
```

```
plt.plot(err_i, toterru, 'blue')
plt.plot(err_i, toterrv, 'red')

labels = [1,2,3,4,5,6,7,8,9,10]
plt.xticks(k_arr,labels)
plt.legend(['Error in u', 'Error in v'])
plt.xlabel('ABL height (x1000)')
plt.ylabel('Error')
plt.grid()
plt.show()
```

B.2. Python code for graph of errors in wind speeds modified linear and with constant vertical wind speed

```
import matplotlib.pyplot as plt
from numpy import sin, cos, exp, sqrt, linspace, array, append, zeros
from bepalingconstanten import *

z = linspace(0, 100000, 100000)
zhat = linspace(0, 1, 100000)

stepsize = 1000
maxi = 1000 / stepsize

toterru = array([])
toterrv = array([])
err_i = array([])

def startderivativepoint(i):
    vzhat = p * exp(zhat[i] * p) * (b1 * cos(zhat[i] * q) + b2 * sin(zhat[
        ↪ i] * q)) + exp(p * zhat[i]) * (
            -b1 * q * sin(q * zhat[i]) + b2 * q * cos(q * zhat[i])) + k *
                ↪ exp(zhat[i] * k) * (
                    b3 * cos(zhat[i] * q) + b4 * sin(zhat[i] * q)) + exp(
                        ↪ zhat[i] * k) * (
                    -b3 * q * sin(q * zhat[i]) + b4 * q * cos(q * zhat[i])
                        ↪ )
    uzhat = -W * ((p ** 2) * exp(p * zhat[i]) * (b1 * cos(zhat[i] * q) +
        ↪ b2 * sin(zhat[i] * q)) + (k ** 2) * exp(
         k * zhat[i]) * (
                            b3 * cos(zhat[i] * q) + b4 * sin(zhat[i] * q)) +
                                ↪  2 * p * exp(p * zhat[i]) * (
                            -b1 * q * sin(q * zhat[i]) + b2 * q * cos(q *
                                ↪ zhat[i])) + 2 * k * exp(k * zhat[i]) * (
                            -b3 * q * sin(q * zhat[i]) + b4 * q * cos(q *
                                ↪ zhat[i])) + exp(p * zhat[i]) * (
                            -b1 * (q ** 2) * cos(q * zhat[i]) - b2 * (q **
                                ↪ 2) * sin(q * zhat[i])) + exp(k * zhat[i])
                                ↪ * (
                            -b3 * (q ** 2) * cos(q * zhat[i]) - b4 * (q **
                                ↪ 2) * sin(q * zhat[i]))) + N * (
                        (p ** 3) * exp(p * zhat[i]) * (b1 * cos(q * zhat[i]) +
                            ↪  b2 * sin(q * zhat[i])) + 3 * (p ** 2) * exp(
                    p * zhat[i]) * (-q * b1 * sin(q * zhat[i]) + b2 * q * cos(
                        ↪ q * zhat[i])) + 3 * p * exp(p * zhat[i]) * (
                                -(q ** 2) * b1 * cos(q * zhat[i]) - (q ** 2) *
                                    ↪  b2 * sin(q * zhat[i])) + exp(p * zhat[i
                                    ↪ ]) * (
                                (q ** 3) * b1 * sin(q * zhat[i]) - b2 * (q **
                                    ↪ 3) * cos(q * zhat[i])) + (k ** 3) * exp(
                    k * zhat[i]) * (b3 * cos(q * zhat[i]) + b4 * sin(q * zhat[
                        ↪ i])) + 3 * (k ** 2) * exp(
                    k * zhat[i]) * (-q * b3 * sin(q * zhat[i]) + b4 * q * cos(
                        ↪ q * zhat[i])) + 3 * k * exp(k * zhat[i]) * (
                                -(q ** 2) * b3 * cos(q * zhat[i]) - (q ** 2) *
                                    ↪  b4 * sin(q * zhat[i])) + exp(k * zhat[i
                                    ↪ ]) * (
```

```
                                (q ** 3) * b3 * sin(q * zhat[i]) - b4 * (q **
                                    ↪ 3) * cos(q * zhat[i])))
    return uzhat,vzhat

def ExplicitEulernonlin(N, W, F, u,v,uz0, vz0, gridpoints, start, endpoint
    ↪ ):
    x1 = zeros([gridpoints])
    y1 = zeros([gridpoints])
    x2 = zeros([gridpoints])
    y2 = zeros([gridpoints])
    x1[0] = u
    y1[0] = v
    x2[0] = uz0
    y2[0] = vz0
    deltat = (endpoint - start) / gridpoints
    for i in range(0, gridpoints - 1):
        x1[i + 1] = x1[i] + deltat * x2[i]
        x2[i + 1] = x2[i] + deltat * (
                    1 / N * (W * x2[i] - y1[i] + F * ((y1[i] / x1[i]) /
                        ↪ sqrt(1 + (y1[i] / x1[i]) ** 2))))
        y1[i + 1] = y1[i] + deltat * y2[i]
        y2[i + 1] = y2[i] + deltat * (1 / N * (W * y2[i] - 1 + x1[i] - F *
            ↪  (1 / sqrt(1 + (y1[i] / x1[i]) ** 2))))
    return x1, y1


for i in range(0, int(maxi) + 1):
    err_u = array([])
    err_v = array([])
    ABL = 2000 + stepsize * i
    ubar = 10
    f = 1.1 * 10 ** (-4)
    Km = 5
    N = Km / (f * ABL ** 2)
    what = 0.0025
    W = (what * ubar) / (f * ABL)
    fhat = 0.9 * 10 ** (-4)
    F = (what * fhat) / f

    Blist = constantebepaling(N, W)

    b1 = Blist[0]
    b2 = Blist[1]
    b3 = -b1
    b4 = Blist[2]

    a = (W ** 2) / (4 * N ** 2)
    b = 1 / N
    r = sqrt(sqrt(a ** 2 + b ** 2))
    concos = np.sqrt((1 + (W ** 2) / (4 * (N ** 2) * (r ** 2))) / 2)
    consin = np.sqrt((1 - (W ** 2) / (4 * (N ** 2) * (r ** 2))) / 2)

    p = (W / (2 * N) + r * concos)
    k = (W / (2 * N) - r * concos)
    q = r * consin
```

```
u = ubar - ubar * exp(-(z * sqrt(f)) / sqrt(2 * Km)) * cos((z * sqrt(f
    ↪ ) / sqrt(2 * Km)))
v = ubar * exp(-(z * sqrt(f)) / sqrt(2 * Km)) * sin((z * sqrt(f)) /
    ↪ sqrt(2 * Km))
uhat = u / ubar
vhat = v / ubar

uw = 1 - W * (p * exp(zhat * p) * (b1 * cos(zhat * q) + b2 * sin(zhat
    ↪ * q)) + exp(p * zhat) * (
        -b1 * q * sin(q * zhat) + b2 * q * cos(q * zhat)) + k * exp(
            ↪ zhat * k) * (
                    b3 * cos(zhat * q) + b4 * sin(zhat * q)) + exp(
                        ↪ zhat * k) * (
                    -b3 * q * sin(q * zhat) + b4 * q * cos(q * zhat)
                        ↪ )) \
     + N * ((p ** 2) * exp(p * zhat) * (b1 * cos(zhat * q) + b2 * sin(
         ↪ zhat * q)) + (k ** 2) * exp(k * zhat) * (
         b3 * cos(zhat * q) + b4 * sin(zhat * q)) + 2 * p * exp(p *
             ↪ zhat) * (
                    -b1 * q * sin(q * zhat) + b2 * q * cos(q * zhat))
                        ↪ + 2 * k * exp(k * zhat) * (
                    -b3 * q * sin(q * zhat) + b4 * q * cos(q * zhat))
                        ↪ + exp(p * zhat) * (
                    -b1 * (q ** 2) * cos(q * zhat) - b2 * (q ** 2) *
                        ↪ sin(q * zhat)) + exp(k * zhat) * (
                    -b3 * (q ** 2) * cos(q * zhat) - b4 * (q ** 2) *
                        ↪ sin(q * zhat)))

vw = exp(zhat * p) * (b1 * cos(zhat * q) + b2 * sin(zhat * q)) + exp(
    ↪ zhat * k) * (
        b3 * cos(zhat * q) + b4 * sin(zhat * q))
vwhat = vw
uwhat = uw

start = 0.01
perturbu = 0.0011
perturbv = 0.00155
endpoint = 1

nonlinearu_arr = array([])
nonlinearv_arr = array([])

q = 0
listi = []
for q in range(0, len(zhat)):
    if zhat[q] > start:
        listi.append(q)

derustart, dervstart = startderivativepoint(min(listi))
nonlinearu_arr = append(nonlinearu_arr, uw[0:min(listi)])
nonlinearv_arr = append(nonlinearv_arr, vw[0:min(listi)])
unonlin, vnonlin = ExplicitEulernonlin(N, W, F, uw[min(listi)], vw[min
    ↪ (listi)], derustart, dervstart, 100000, start,
                                       endpoint)

nonlinearu_arr = append(nonlinearu_arr, unonlin)
```

```
    nonlinearv_arr = append(nonlinearv_arr, vnonlin)

    for j in range(len(vhat)):
        err_v = append(err_v, abs(vwhat[j] - nonlinearv_arr[j]))

    for j in range(len(uhat)):
        err_u = append(err_u, abs(uwhat[j] - nonlinearu_arr[j]))

    print(sum(err_u))

    toterru = append(toterru, sum(err_u))
    toterrv = append(toterrv, sum(err_v))
    err_i = append(err_i, i)
    print(err_i)
    print(ABL)

k_arr = array([])
for k in range(0, len(err_i)):
    if int(1000 + stepsize * err_i[k]) % 1000 == 0:
        k_arr = append(k_arr, k)

plt.plot(err_i, toterru, 'blue')
plt.plot(err_i, toterrv, 'red')

#labels = [1,2,2.5]
#plt.xticks(k_arr,labels)
plt.legend(['Error in u', 'Error in v'])
plt.xlabel('ABL height (x1000)')
plt.ylabel('Error')
plt.grid()
plt.savefig('eskettitcomparison')
plt.show()
```

C

Visualizing the Classical Ekman Spiral

```
from numpy import sin, cos, exp, sqrt, linspace, seterr, set_printoptions
import matplotlib.pyplot as plt
from bepalingconstanten import *
import sys

seterr(all='ignore')
set_printoptions(threshold=sys.maxsize)

z = linspace(0, 100000, 100000)
zhat = linspace(0, 1, 100000)

ABL = 2500
ubar = 10
f = 1.1 * 10 ** (-4)
Km = 5

u = ubar - ubar * exp(-(z * sqrt(f)) / sqrt(2 * Km)) * cos((z * sqrt(f) /
    ↪ sqrt(2 * Km)))
v = ubar * exp(-(z * sqrt(f)) / sqrt(2 * Km)) * sin((z * sqrt(f)) / sqrt(2
    ↪  * Km))

ax = plt.axes()
ubarstr = "u" + u"\u0304"
uhatstr = "u" + u"\u0302"
vhatstr = "v" + u"\u0302"

plt.xlabel(uhatstr)
plt.ylabel(vhatstr)
plt.grid()
plt.plot(u, v, 'blue')

plt.plot(u[10], v[10], 'ro')
plt.plot(u[100], v[100], 'go')
plt.plot(u[1000], v[1000], 'mo')
plt.plot(u[10000], v[10000], 'ko')

plt.show()
```

D

Visualizing the Modified Linear Ekman Spiral

```
from numpy import sin, cos, exp, sqrt, linspace, seterr, array, append,
    ↪ arange, vstack
import matplotlib.pyplot as plt
from bepalingconstanten import *



seterr(all='ignore')

step = 500000
z = linspace(0,10000,step)
zhat = linspace(0,1,step)

datau = array([zhat])
datav = array([zhat])

j = 0
ABL = 1020
what = 0.005
ubar = 10
f = 1.1 * 10 ** (-4)
Km = 5

W_arr = array([])
legend_arr = ([])


uhatstr = "u" + u"\u0302"
vhatstr = "v" + u"\u0302"
whatstr = "w" + u"\u0302"

for W in arange(0.01,0.04,0.01):

    W_arr = append(W_arr,W)
    str1 = "W = " + str(W_arr[j])
    legend_arr = append(legend_arr, str1)
    j += 1
```

```
N = Km / (f * ABL ** 3)

Blist = constantebepaling(N, W)
b1 = Blist[0]
b2 = Blist[1]
b3 = -b1
b4 = Blist[2]

a = (W ** 2) / (4 * N ** 2)
b = 1 / N
r = sqrt(sqrt(a ** 2 + b ** 2))
concos = sqrt((1 / 2) * (1 + (a) / (r ** 2)))
consin = sqrt((1 / 2) * (1 - (a) / (r ** 2)))

p = (W / (2 * N) + r * concos)
k = (W / (2 * N) - r * concos)
q = r * consin

u = ubar - ubar * exp(-(z * sqrt(f)) / sqrt(2 * Km)) * cos((z * sqrt(f
    ↪ ) / sqrt(2 * Km)))
v = ubar * exp(-(z * sqrt(f)) / sqrt(2 * Km)) * sin((z * sqrt(f)) /
    ↪ sqrt(2 * Km))
uhat = u / ubar
vhat = v / ubar

uw = 1 - W * (p * exp(zhat * p) * (b1 * cos(zhat * q) + b2 * sin(zhat
    ↪ * q)) + exp(p * zhat) * (
            -b1 * q * sin(q * zhat) + b2 * q * cos(q * zhat)) + k *
                ↪ exp(zhat * k) * (
                        b3 * cos(zhat * q) + b4 * sin(zhat * q)) +
                            ↪ exp(zhat * k) * (
                        -b3 * q * sin(q * zhat) + b4 * q * cos(q *
                            ↪ zhat))) \
     + N * ((p ** 2) * exp(p * zhat) * (b1 * cos(zhat * q) + b2 * sin(
         ↪ zhat * q)) + (k ** 2) * exp(k * zhat) * (
            b3 * cos(zhat * q) + b4 * sin(zhat * q)) + 2 * p * exp(p *
                ↪  zhat) * (
                    -b1 * q * sin(q * zhat) + b2 * q * cos(q *
                        ↪ zhat)) + 2 * k * exp(k * zhat) * (
                    -b3 * q * sin(q * zhat) + b4 * q * cos(q *
                        ↪ zhat)) + exp(p * zhat) * (
                    -b1 * (q ** 2) * cos(q * zhat) - b2 * (q ** 2)
                        ↪  * sin(q * zhat)) + exp(k * zhat) * (
                    -b3 * (q ** 2) * cos(q * zhat) - b4 * (q ** 2)
                        ↪  * sin(q * zhat)))

vw = exp(zhat * p) * (b1 * cos(zhat * q) + b2 * sin(zhat * q)) + exp(
    ↪ zhat * k) * (
            b3 * cos(zhat * q) + b4 * sin(zhat * q))
vwhat = vw
uwhat = uw

uwhat_array = array(uwhat)
vwhat_array = array(vwhat)
```

```
    datau = vstack([datau,uwhat_array])
    datav = vstack([datav,vwhat_array])


color_arr = array(['black','blue','red','green','orange','purple','
    ↪ mediumaquamarine','grey','brown'])

for i in range(1,j+1):
    plt.plot(datau[i],datav[i],color_arr[i-1])
    print(legend_arr[i-1])

plt.grid()
plt.legend(legend_arr)
plt.xlabel(uhatstr)
plt.ylabel(vhatstr)

# plt.savefig('ModLinDiffWcloseup')
plt.show()
```

E

Visualizing the Ekman Spiral with Vertical Wind Speed

```
from numpy import sin, cos, exp, sqrt, linspace, seterr, asarray, zeros,
    ↪ arange, array, append
from bepalingconstanten import *
import matplotlib.pyplot as plt

seterr(all='ignore')


def startderivativepoint(i):
    vzhat = p * exp(zhat[i] * p) * (b1 * cos(zhat[i] * q) + b2 * sin(zhat[
        ↪ i] * q)) + exp(p * zhat[i]) * (
            -b1 * q * sin(q * zhat[i]) + b2 * q * cos(q * zhat[i])) + k *
                ↪ exp(zhat[i] * k) * (
                    b3 * cos(zhat[i] * q) + b4 * sin(zhat[i] * q)) + exp(
                        ↪ zhat[i] * k) * (
                    -b3 * q * sin(q * zhat[i]) + b4 * q * cos(q * zhat[i])
                        ↪ )
    uzhat = -W * ((p ** 2) * exp(p * zhat[i]) * (b1 * cos(zhat[i] * q) +
        ↪ b2 * sin(zhat[i] * q)) + (k ** 2) * exp(
         k * zhat[i]) * (
                            b3 * cos(zhat[i] * q) + b4 * sin(zhat[i] * q)) +
                                ↪  2 * p * exp(p * zhat[i]) * (
                            -b1 * q * sin(q * zhat[i]) + b2 * q * cos(q *
                                ↪ zhat[i])) + 2 * k * exp(k * zhat[i]) * (
                            -b3 * q * sin(q * zhat[i]) + b4 * q * cos(q *
                                ↪ zhat[i])) + exp(p * zhat[i]) * (
                            -b1 * (q ** 2) * cos(q * zhat[i]) - b2 * (q **
                                ↪ 2) * sin(q * zhat[i])) + exp(k * zhat[i])
                                ↪ * (
                            -b3 * (q ** 2) * cos(q * zhat[i]) - b4 * (q **
                                ↪ 2) * sin(q * zhat[i]))) + N * (
                        (p ** 3) * exp(p * zhat[i]) * (b1 * cos(q * zhat[i]) +
                            ↪  b2 * sin(q * zhat[i])) + 3 * (p ** 2) * exp(
                    p * zhat[i]) * (-q * b1 * sin(q * zhat[i]) + b2 * q * cos(
                        ↪ q * zhat[i])) + 3 * p * exp(p * zhat[i]) * (
                                -(q ** 2) * b1 * cos(q * zhat[i]) - (q ** 2) *
                                    ↪  b2 * sin(q * zhat[i])) + exp(p * zhat[i
```

```
                                ↪ ]) * (
                            (q ** 3) * b1 * sin(q * zhat[i]) - b2 * (q **
                                ↪ 3) * cos(q * zhat[i])) + (k ** 3) * exp(
                    k * zhat[i]) * (b3 * cos(q * zhat[i]) + b4 * sin(q * zhat[
                        ↪ i])) + 3 * (k ** 2) * exp(
                    k * zhat[i]) * (-q * b3 * sin(q * zhat[i]) + b4 * q * cos(
                        ↪ q * zhat[i])) + 3 * k * exp(k * zhat[i]) * (
                                -(q ** 2) * b3 * cos(q * zhat[i]) - (q ** 2) *
                                ↪  b4 * sin(q * zhat[i])) + exp(k * zhat[i
                                ↪ ]) * (
                            (q ** 3) * b3 * sin(q * zhat[i]) - b4 * (q **
                                ↪ 3) * cos(q * zhat[i])))
    return uzhat,vzhat

def ExplicitEulernonlin(N, W, F, u,v,uz0, vz0, gridpoints, start, endpoint
    ↪ ):
    x1 = zeros([gridpoints])
    y1 = zeros([gridpoints])
    x2 = zeros([gridpoints])
    y2 = zeros([gridpoints])
    x1[0] = u
    y1[0] = v
    x2[0] = uz0
    y2[0] = vz0
    deltat = (endpoint - start) / gridpoints
    for i in range(0, gridpoints - 1):
        x1[i + 1] = x1[i] + deltat * x2[i]
        x2[i + 1] = x2[i] + deltat * (
                    1 / N * (W * x2[i] - y1[i] + F * ((y1[i] / x1[i]) /
                        ↪ sqrt(1 + (y1[i] / x1[i]) ** 2))))
        y1[i + 1] = y1[i] + deltat * y2[i]
        y2[i + 1] = y2[i] + deltat * (1 / N * (W * y2[i] - 1 + x1[i] - F *
            ↪  (1 / sqrt(1 + (y1[i] / x1[i]) ** 2))))
    return x1, y1

fhat = 0.9*10**(-4)
ABL = 1000
what = 0.0025
ubar = 20
f = 1.1 * 10 ** (-4)
Km = 5
N = Km/(f*ABL**(2))
W = ubar/(ABL*f)*what
F = (what*fhat)/f


start= 0.01
perturbu = 0
perturbv = 0.00155
endpoint = 1

loop_arr = array([])
legend_arr = ([])

z = linspace(0, 10000, 50000)
zhat = linspace(0, 1, 500000)
```

```
datau = [zhat]
datav = [zhat]


uhatstr = "u" + u"\u0302"
vhatstr = "v" + u"\u0302"
whatstr = "w" + u"\u0302"

j=0
i_arr = array([])

for perturbu in arange(0.0011,0.003,0.05):
    loop_arr = append(loop_arr, round(perturbu,4))
    str1 = str(loop_arr[j])
    legend_arr = append(legend_arr, str1)
    j += 1

    a = (W ** 2) / (4 * N ** 2)
    b = 1 / N
    r = sqrt(sqrt(a ** 2 + b ** 2))
    concos = sqrt((1 / 2) * (1 + (a) / (r ** 2)))
    consin = sqrt((1 / 2) * (1 - (a) / (r ** 2)))

    p = (W / (2 * N) + r * concos)
    k = (W / (2 * N) - r * concos)
    q = r * consin

    Blist = constantebepaling(N, W)
    b1 = Blist[0]
    b2 = Blist[1]
    b3 = -b1
    b4 = Blist[2]

    vz0 = b1 * p + b2 * q + b3 * k + b4 * q
    uz0 = N * (
                b1 * p ** 3 - 3 * b1 * p * q ** 2 + 3 * b2 * p ** 2 * q -
                    ↪ b2 * q ** 3 + b3 * k ** 3 - 3 * b3 * k * q ** 2 + 3
                    ↪ * b4 * k ** 2 * q - b4 * q ** 3) - W * (
                       b1 * p ** 2 - b1 * q ** 2 + 2 * b2 * p * q + b3 * k
                           ↪ ** 2 - b3 * q ** 2 + 2 * b4 * k * q)


    vzhat = p * exp(zhat * p) * (b1 * cos(zhat * q) + b2 * sin(zhat * q))
       ↪ + exp(p * zhat) * (
            -b1 * q * sin(q * zhat) + b2 * q * cos(q * zhat)) + k * exp(
               ↪ zhat * k) * (
                    b3 * cos(zhat * q) + b4 * sin(zhat * q)) + exp(zhat *
                       ↪ k) * (
                    -b3 * q * sin(q * zhat) + b4 * q * cos(q * zhat))
    uzhat = -W * ((p ** 2) * exp(p * zhat) * (b1 * cos(zhat * q) + b2 *
       ↪ sin(zhat * q)) + (k ** 2) * exp(k * zhat) * (
            b3 * cos(zhat * q) + b4 * sin(zhat * q)) + 2 * p * exp(p *
               ↪ zhat) * (
                       -b1 * q * sin(q * zhat) + b2 * q * cos(q * zhat)
                          ↪ ) + 2 * k * exp(k * zhat) * (
```

```
                    -b3 * q * sin(q * zhat) + b4 * q * cos(q * zhat)
                       ↪ ) + exp(p * zhat) * (
                    -b1 * (q ** 2) * cos(q * zhat) - b2 * (q ** 2) *
                       ↪  sin(q * zhat)) + exp(k * zhat) * (
                    -b3 * (q ** 2) * cos(q * zhat) - b4 * (q ** 2) *
                       ↪  sin(q * zhat))) + N * (
                (p ** 3) * exp(p * zhat) * (b1 * cos(q * zhat) +
                   ↪ b2 * sin(q * zhat)) + 3 * (p ** 2) * exp(
            p * zhat) * (-q * b1 * sin(q * zhat) + b2 * q * cos(q
               ↪ * zhat)) + 3 * p * exp(p * zhat) * (
                                -(q ** 2) * b1 * cos(q * zhat) - (q **
                                   ↪  2) * b2 * sin(q * zhat)) + exp(
                                   ↪ p * zhat) * (
                                (q ** 3) * b1 * sin(q * zhat) - b2 * (
                                   ↪ q ** 3) * cos(q * zhat)) + (k **
                                   ↪  3) * exp(k * zhat) * (b3 * cos(
                                   ↪ q * zhat) + b4 * sin(q * zhat))
                                   ↪ + 3 * (k ** 2) * exp(
            k * zhat) * (-q * b3 * sin(q * zhat) + b4 * q * cos(q
               ↪ * zhat)) + 3 * k * exp(k * zhat) * (
                                -(q ** 2) * b3 * cos(q * zhat) - (q **
                                   ↪  2) * b4 * sin(q * zhat)) + exp(
                                   ↪ k * zhat) * (
                                (q ** 3) * b3 * sin(q * zhat) - b4 * (
                                   ↪ q ** 3) * cos(q * zhat)))

uexact = ubar - ubar * exp(-(z * sqrt(f)) / sqrt(2 * Km)) * cos((z *
   ↪ sqrt(f) / sqrt(2 * Km)))
vexact = ubar * exp(-(z * sqrt(f)) / sqrt(2 * Km)) * sin((z * sqrt(f))
   ↪  / sqrt(2 * Km))
uhat = uexact / ubar
vhat = vexact / ubar

uw = perturbu + 1 - W * (p * exp(zhat * p) * (b1 * cos(zhat * q) + b2
   ↪ * sin(zhat * q)) + exp(p * zhat) * (
        -b1 * q * sin(q * zhat) + b2 * q * cos(q * zhat)) + k * exp(
           ↪ zhat * k) * (
                    b3 * cos(zhat * q) + b4 * sin(zhat * q)) + exp(
                       ↪ zhat * k) * (
                    -b3 * q * sin(q * zhat) + b4 * q * cos(q * zhat)
                       ↪ )) \
     + N * ((p ** 2) * exp(p * zhat) * (b1 * cos(zhat * q) + b2 * sin(
        ↪ zhat * q)) + (k ** 2) * exp(k * zhat) * (
        b3 * cos(zhat * q) + b4 * sin(zhat * q)) + 2 * p * exp(p *
           ↪ zhat) * (
                -b1 * q * sin(q * zhat) + b2 * q * cos(q * zhat))
                   ↪ + 2 * k * exp(k * zhat) * (
                -b3 * q * sin(q * zhat) + b4 * q * cos(q * zhat))
                   ↪ + exp(p * zhat) * (
                -b1 * (q ** 2) * cos(q * zhat) - b2 * (q ** 2) *
                   ↪ sin(q * zhat)) + exp(k * zhat) * (
                -b3 * (q ** 2) * cos(q * zhat) - b4 * (q ** 2) *
                   ↪ sin(q * zhat)))

vw = perturbv + exp(zhat * p) * (b1 * cos(zhat * q) + b2 * sin(zhat *
   ↪ q)) + exp(zhat * k) * (
```

```
            b3 * cos(zhat * q) + b4 * sin(zhat * q))
    vwhat = vw
    uwhat = uw

    nonlinearu_arr = array([])
    nonlinearv_arr = array([])

    i = 0
    listi=[]
    for i in range(0,len(zhat)):
        if zhat[i] > start:
            listi.append(i)
    i_arr = append(i_arr,int(min(listi)))

    derustart, dervstart = startderivativepoint(min(listi))
    nonlinearu_arr = append(nonlinearu_arr, uw[0:min(listi)])
    nonlinearv_arr = append(nonlinearv_arr, vw[0:min(listi)])
    unonlin,vnonlin = ExplicitEulernonlin(N,W,F,uw[min(listi)],vw[min(
        ↪ listi)],derustart,dervstart,100000,start,endpoint)

    nonlinearu_arr = append(nonlinearu_arr,unonlin)
    nonlinearv_arr = append(nonlinearv_arr, vnonlin)

    datau.append(nonlinearu_arr)
    datav.append(nonlinearv_arr)

datau = asarray(datau)
datav = asarray(datav)
color_arr = array(['black','blue','red','green','orange','purple','
    ↪ mediumaquamarine','grey','brown'])
for i in range(1,j+1):
    plt.plot(datau[i],datav[i],color_arr[i-1])
plt.grid()
#plt.legend(legend_arr)
for i in range(1,j+1):
    print(i_arr[i-1])
    plt.plot(datau[i][int(i_arr[i-1])], datav[i][int(i_arr[i-1])], 'o',
        ↪ color = color_arr[i - 1])
plt.xlabel(uhatstr)
plt.ylabel(vhatstr)
# plt.savefig('NonLinDiffFinal0t')
plt.show()
```